

Chapter 1 – Introduction

1.1 Introduction

The main aim of the work reported in this thesis is to shed light on the elusive nature of RF discharges and to gain a better understanding of the factors controlling etch processes, in particular sidewall profiles, etch rates and substrate damage. This thesis concerns a detailed study of the energies that ions, electrons and neutral atoms possess in dry etch processes. The work consists of three separate sections.

Firstly, there is a detailed experimental study of optical emission linewidths from excited Cl and Ga atoms during the reactive ion etching of GaAs in Cl-based plasmas. This yields information about the kinetic energies possessed by some neutral species in the plasma, and points to some of the chemical processes that are occurring within the bulk of the discharge.

Secondly, a theoretical investigation is undertaken of the energies that positive ions obtain as they are accelerated through the sheath potential to strike the substrate. A thorough study of the energy distributions for ions arriving at the cathode of a reactive ion etcher is performed, since it is known that high energy ion bombardment of the semiconductor surface plays a central role in etch mechanisms. The inherent directionality of these ion trajectories is one of the mechanisms for anisotropic etching and is thus an essential feature of submicron pattern delineation in VLSI and ULSI. The approach adopted is to develop a model for the sheath region and then use a Monte Carlo computer program to calculate the trajectories of ions passing through this sheath until they strike the electrode. Collisional interactions between the ions and neutral species within the sheath have also been modelled, which allows extension of the simulations to include high pressure plasmas. The energy distributions calculated in this fashion are then compared to available experimental data. The program is extended to simulate the energies of other particles, such as electrons and fast neutrals, since these energies are also crucial to etch processes.

Finally, using the results from these simulations, another program is used to simulate the sidewall profile expected when sputtering an amorphous Si substrate with Ar^+ ions. The results from this simulation are compared to experimental observations and found to reproduce the basic trends seen when Si is etched under a variety of different Ar plasma conditions.

Having outlined the aims of this work, the way in which semiconductors such as Si and GaAs are used in the fabrication of integrated circuits is now described.

1.2 Integrated Circuits

An integrated circuit (IC) is a group of inseparably connected circuit elements fabricated in place, on and within a substrate or wafer. The most commonly used substrates are Si [1] and GaAs [2].

The first integrated circuit was made by Kilby [3] at Texas Instruments by a technique known as the *planar process*. This process was subsequently developed early in 1959 by Noyce and Moore [4] at Fairchild Semiconductor and is now the major production method for Si microelectronic circuits.

GaAs integrated circuits were first manufactured by Hewlett Packard in 1974 [5]. GaAs has a

number of physical properties which give it advantages over and the number of devices which incorporate GaAs is therefore increasing rapidly. Although GaAs devices use slightly different principles to Si ones, their manufacturing processes are similar. Descriptions of the fabrication processes for GaAs devices can be found in ref.[1,6-8].

1.2.1 Planar Processing

Planar processing involves the fabrication of layers of semiconducting materials, one on top of the other, to form a multi-layered 'sandwich'. A typical IC may consist of up to 15 layers, requiring as many as 200 process steps. Each layer is made of a material with precisely controlled electrical properties. These layers are then patterned such that the entire sandwich forms the various circuit elements, such as resistors, capacitors and rectifiers. These are finally connected together by a patterned conducting layer (the interconnect), usually composed of an Al alloy.

1.2.2 Starting Materials

Both Si and GaAs ICs are fabricated on single crystal wafers. Si wafers are manufactured from raw silica which is purified and *zone refined* [1]. Single crystal ingots are first grown by the *Czochralski* [18] or the *floating zone* [19] method. The ingot is then sawn into wafers, which are lapped, polished and chemically etched to produce a mirror finish. Si wafers are usually about 0.5-mm thick, although much thinner ones are also produced. Their diameter has grown from 75 mm to 200 mm over the last ten years.

GaAs is grown via the *Horizontal Bridgman* [2] or *Liquid Encapsulated Czochralski* [2,10] methods. Cr is often added as a compensating dopant to mop up any Si contaminant. The ingots are sawn into wafers, polished and chemically treated in a similar manner to Si wafers. GaAs wafers must be at least 0.5 mm thick to avoid damage in handling. Due to the inherent difficulties in manufacture, their diameter rarely exceeds 75 mm.

1.2.3 Process Steps

There are four main process steps required to produce a patterned layer in an integrated circuit: film production, doping, photolithography and etching. These four basic steps are repeated many times to build up the complex multi-layered structure of a modern Si chip. In order to understand the role played by dry etching in IC fabrication, a brief overview of these four steps is given below.

1.2.3.1 Film Formation

A primary requirement in each cycle of the IC fabrication process is the ability to produce thin films of the required material. Apart from oxidation of the substrate Si (carried out in an

oven with O₂ or steam flowing through it), all other layers must be deposited by different means. Deposition by any technique requires the controlled formation of involatile species at a surface. Deposited films generally require the following properties:

- a) Good adhesion to the underlying layer.
- b) Good thickness uniformity.
- c) Controlled stoichiometry and film composition.
- d) Few contaminants.
- e) Good step coverage.
- f) Compatibility with subsequent process steps.
- g) Unreactivity to adjacent layers.
- h) If the film is permanent, it must be durable. If a film is only temporary (*e.g.* photoresist) it must be easy to remove.

There are many methods to produce the thin films that are used in the various process steps during IC fabrication. Only a brief description of some of them is given here. A more detailed account can be found in ref.[9,10].

1.2.3.1.1 Spin-on and Spray-on Processes

The reagents are dissolved in a carrier liquid which is sprayed (or spun) onto the heated substrate. When the solvent evaporates it leaves the remaining components to react together at the surface. This is sometimes achieved in a high temperature heating step. Due to the difficulties of controlling chemical composition, thickness uniformity, step coverage and bubbling, these techniques are rarely used nowadays except for the application of photoresist [10].

1.2.3.1.2 Chemical Vapour Deposition (CVD)

This is the major method for producing thin films, since films of most materials can be produced in this way [11]. In CVD, gas-phase species react at a heated substrate surface to form an involatile product. Each gas is independently variable in concentration, so that the stoichiometry of the film can be accurately controlled [12]. CVD can be performed at Atmospheric Pressure (APCVD) or Low Pressure, 0.1-1 Torr (LPCVD), with each pressure regime having advantages and disadvantages over the other [13]. A more recent development has been Plasma Enhanced CVD (PECVD) where a glow discharge plasma provides a means of augmenting the low deposition rates of standard LPCVD processes [14,17].

1.2.3.1.3 Sputtering [10]

In this technique, high energy inert gas ions (usually Ar⁺) created by an ion gun or discharge source inside a vacuum chamber, strike a target composed of the material to be sputtered. Momentum transfer causes particles of the target to be ejected at high velocity into the chamber,

where they adhere to adjacent surfaces. The substrate to be coated is placed close to the target and is covered in sputtered particles so that a thin film slowly builds up. The substrate is often heated to increase adhesion of the film and to control stoichiometry and grain size. The ion source can either be an ion gun or a plasma discharge. This technique is often used for deposition of metallic layers, since it gives good uniformity and step coverage.

1.2.3.1.4 Evaporation [10]

This is a common method used to produce metallic films. A pellet of the material to be evaporated is placed in a crucible inside a vacuum chamber. When the crucible is heated by electron bombardment or by passing an electrical current through it, the material evaporates and coats a nearby substrate. By using separate crucibles containing pellets of different materials, alloy films can be co-evaporated.

1.2.3.1.5 Miscellaneous Techniques

Films with complex stoichiometries can be produced by more exotic techniques. *Laser Ablation* uses a focused, high power laser beam to heat a pellet of the material at a localised spot, causing thermal evaporation and coating of a nearby substrate. This technique has recently been used to produce thin films of the new high temperature superconducting material [17].

Other techniques include *Molecular Beam Epitaxy* (MBE) and *Metal-Organic CVD* (MOCVD). MBE is the growth of elemental, compound and alloy films by the impingement of directed thermal energy atomic or molecular beams on a crystalline surface under UHV conditions [21,22]. MOCVD involves the pyrolysis of a vapour-phase mixture of reactants which includes a volatile organo-metallic reagent [23,24].

1.2.3.2. Doping and Implantation

Once the film has been produced, it is necessary to ensure that it has the correct degree and type of electrical conductivity for its purpose. It is often necessary to add impurities or dopants into the film to adjust the electrical conductivity. Until recently this was achieved by high temperature diffusion techniques. A layer of the dopant material was deposited on the film surface, and then followed by a *drive-in* step in which the wafers were placed in a furnace (at about 1000°C) to allow solid-state diffusion of the impurities to take place.

However as IC dimensions have decreased, the requirements for precise control of these impurity levels has led to the adoption of *ion implantation* as the predominant technique for the selective introduction of dopant impurities. This technique is accomplished by bombarding the substrate surface with a beam of ions whose energy is in the range one to several hundred keV. Areas not to be implanted are usually covered with a masking material, such as photoresist or SiO₂. Ion implantation gives several advantages:

- (a) Precise control of impurity concentrations.
- (b) Control of impurity profile.

- (c) A wide range of suitable mask materials is available.
- (d) It is a low temperature technique.

and disadvantages:

- (a) Complex, extremely expensive equipment using UHV techniques is required.
- (b) Heavy implant doses can produce damage to the crystal lattice, although this can often be repaired by a subsequent anneal step.

A typical implantation step is to introduce B⁺ ions into the Si lattice to produce a p-type layer [25].

1.2.3.3 Photolithography

This step defines the pattern that will subsequently be transferred into the layer during the later etch step. The wafers are coated with an ultra-violet light-sensitive chemical called a *photoresist* (or simply resist). This can be classed as either positive or negative [25]. With positive resists, those regions exposed to the UV-light may be developed and removed, while the unexposed regions remain insoluble in the developer. Negative resists behave in the opposite fashion. The wafers are baked to harden the resist and then aligned to a photomask carrying the required etch pattern. The wafer is then illuminated with UV-light through the mask to print the pattern [25]. The pattern is developed by placing the wafer into contact with a developing fluid which chemically attacks and removes the exposed (or unexposed) regions. This leaves the image behind to serve as a mask for etching. Features on the resist mask are typically 2-3 μm high and <1-100 μm wide, with a near vertical sidewall.

The patterned wafer is then baked to harden the resist sufficiently to withstand the harsh etching environment that follows. This bake normally consists of a '*soft-bake*' in an oven at ~100°C, which is sufficient for most etch processes. Some etch processes however, are particularly damaging to the resist, and in these cases a higher temperature bake is required to harden the resist further. Unfortunately most resists 'flow' (or melt) at temperatures ~120°C so another step is added before the bake. The wafers are exposed to deep UV (DUV) for approximately 30 mins to produce a hard-shell coating of polymerised resist around the features. This now enables the wafers to be baked at temperatures of up to 180°C without loss of feature definition, making the resist harder and more etch resistant. This process is known as *DUV hardening*.

After the subsequent etch process the resist is removed, either by a chemical bath (such as fuming nitric acid) or exposure to an O₂ plasma (a so-called *ash* step).

1.2.3.4 Etching

Etching is the removal of atoms from the film surface. The atoms removed will only be those that are exposed to the etching medium, that is those that are not covered by the photoresist

mask. The basic requirements of an etch process are:

- (a) Removal of the surface atoms.
- (b) Selectivity to any surfaces or layers that are not to be etched.
- (c) Accurate pattern transfer from the mask to the substrate.
- (d) No residues, *i.e.* a clean process.

The two main etch techniques in use today are called *wet* and *dry etching*, and these are discussed below.

1.2.3.4.1 Wet Etching

This involves immersion of the wafer into a solution of the required chemicals for an appropriate length of time. Dissolution of the film occurs, whilst agitation of the solution allows a constant supply of fresh reactant to reach the etching region. Although wet etching techniques can be extremely selective, they often suffer from being *isotropic* in nature. This means that the depth of the etch approximates to the amount of lateral etching, since etching proceeds at about the same rate in all directions (see fig.1.1). Consequently etching a 1 μm -thick film would also result in undercutting the resist mask by $\sim 1 \mu\text{m}$. This would be acceptable for a large device feature ($>10 \mu\text{m}$), but as device dimensions approach 1 μm , wet etching rapidly becomes an unrealistic prospect. The need for a directional, vertical, or *anisotropic* etch has led to the adoption of dry etching as the predominant technique in the modern semiconductor industry. Nowadays wet etching is only used for resist removal, cleans or large-dimension etch steps. A review by Elliott [10] thoroughly discusses wet etching methods.

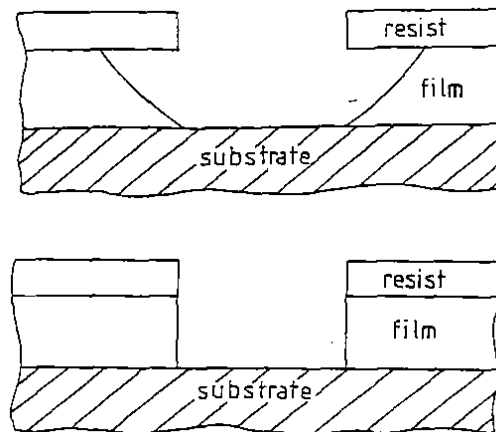


Fig.1.1. Isotropic (top) and Anisotropic (bottom) etching.

1.2.3.4.2 Dry Etching

These processes have evolved as a direct result of the inability of wet etching processes to achieve the high dimensional accuracy required in VLSI. Given a correct process, near fully

anisotropic etching can result, although most real processes do exhibit some degree of isotropy and produce slight mask undercut.

The advantages of dry etching over wet etching are:

- i) Delineation of submicron features becomes possible.
- ii) Reduced undercutting of masks, *i.e.* it is an anisotropic process.
- iii) Abrupt termination of the etch once the power source is turned off.
- iv) Elimination of waste acid disposal problems.
- v) Safer processing, since fewer dangerous chemicals are involved.
- vi) Dry processing eliminates the need for wet-benches in fabrication laboratories.

However dry etching has a few disadvantages also:

- i) Very expensive equipment is required.
- ii) Less selectivity to underlying layers.
- iii) Possible damage to the semiconductor lattice by high energy ion bombardment.
- iv) Lattice crystal planes are not easily distinguished.

Dry etching techniques are generally categorised into three main types depending upon the relative amounts of physical and chemical processes occurring at the substrate surface. These processes go by the names of *ion beam etching*, *plasma etching* and *reactive ion etching*. All of these techniques use gas discharges to produce energetic species that facilitate the etching by physical or chemical means. A detailed description of these dry etching techniques is given in section 1.3.

1.2.3.4.3 Miscellaneous Techniques

There are a few other methods of etching which are occasionally used for specialised purposes. Some of these are adaptations of the basic dry etching technology.

Triode etchers [47] are similar to normal RF reactors, except that they utilise two RF generators at different frequencies. There can be many geometries and configurations for triode reactors, but a typical application is to power the walls of the chamber at 13.56 MHz, and one electrode at 100 kHz, with the other electrode remaining grounded. The high frequency RF is used to produce and maintain the discharge, whilst the lower frequency RF on the cathode is used to accelerate ions onto the wafer. In theory, this allows the chemical reactions in the plasma bulk and the ion bombardment energy to be independently controlled and varied.

Electron Cyclotron Resonance (ECR) reactors use RF or microwave discharges to initiate the plasma, but contain it within a strong magnetic field [36]. This causes the electrons to follow spiral paths and therefore undergo far more collisions than in typical RF reactors. Consequently, the degree of ionisation is higher in these reactors, and so they can work at much lower pressures (<1 mTorr). This provides very anisotropic etching with minimum damage.

Laser-Induced etching [37] utilises a powerful laser to decompose reactive gas reagents above the surface of a wafer, increasing the etch rate from that seen using other techniques. *Direct Laser Writing* [38] uses a high powered laser beam that is tightly focused to a small spot

on the substrate surface. The energy density at the spot is so high that local evaporation of the surface takes place. By scanning the beam across the wafer, the required complex patterns can be produced.

1.2.4 MOS Transistors

We shall now briefly examine some aspects of a typical electronic device that is produced by the sequential implementation of the fabrication processes discussed in the previous sections. We shall concentrate on *Metal-Oxide Semiconductor* (MOS) technology, since these devices dominate IC production at the present time. The technology gets its name from the basic structure of a metal electrode (the gate) over an oxide dielectric over a semiconductor substrate[35]. The name is a slight misnomer since the 'metal' gate is nowadays made from highly-doped polycrystalline Si which is a good electrical conductor. A typical n-channel MOS transistor is shown in fig.1.2. Between two highly-doped regions (the *source* and *drain*) is a lightly-doped channel. Above this channel is an electrode (the *gate*), insulated from the semiconductor surface by an oxide barrier. If a sufficiently positive voltage is applied to the gate, electrons from the substrate bulk are attracted into the channel. This shorts the source and drain allowing current to flow between them. The device so-formed constitutes a transistor, and so possesses two invaluable attributes:

- i) It can act as a very fast switch. Coupling many of these devices together in logic arrays leads to digital electronics and computers.
- ii) Since the small gate voltage (~5 V) controls a large source-drain voltage (tens of Volts), the device can operate as an amplifier.

MOS transistors are very fast, use very little power and are relatively cheap to produce. The latter is true as a result of planar processing, whereby millions of these transistors are created simultaneously on a single piece of Si.

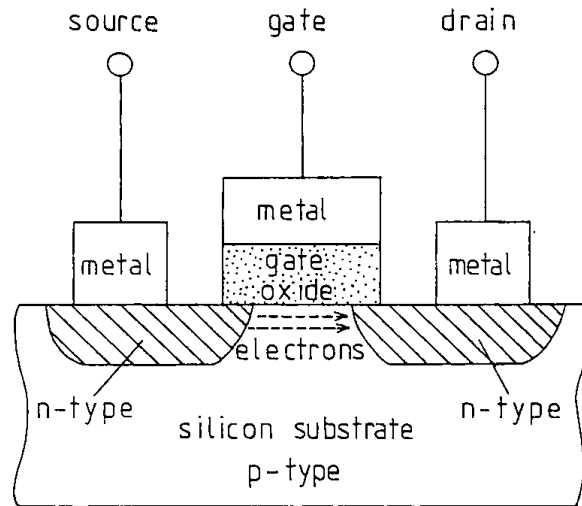


Fig.1.2. Diagram of a typical n-channel MOS transistor (after Elliott [10]). If a sufficiently positive voltage is supplied to the gate, a conducting pathway is formed between source and drain.

1.2.4.1 MOS Transistor Fabrication

A typical process sequence for one stage of the fabrication process is illustrated in fig.1.3. This produces the gate electrode from polycrystalline Si.

- (a) The Si wafer is cleaned, and a thin layer of oxide ($\sim 400 \text{ \AA}$) is grown by thermal oxidation. PolySi ($0.5\text{-}1 \mu\text{m}$) is deposited by CVD and then highly-doped by controlled diffusion of P in an oven.
- (b) A photoresist layer is applied and baked, then the wafer is exposed to UV-light through a mask to define the gate.
- (c) The resist is developed to leave the required pattern.
- (d) The exposed polySi surface is etched away, stopping on the oxide layer.
- (e) P^+ ions are implanted through the thin oxide layer into the Si to form the source and drain regions either side of the gate.
- (f) The resist is removed leaving the completed structure.

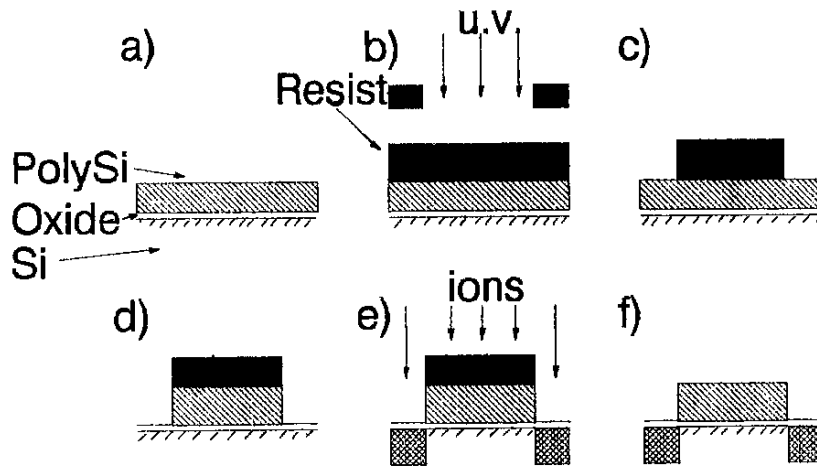


Fig.1.3. typical process sequence for MOS fabrication. This shows the delineation of the gate electrode.

It must be emphasised that this procedure only produces one layer of a multi-layered device. Subsequent steps isolate the separate transistors, cover them with an insulating dielectric film, etch contact holes to the source, gate and drain regions, join the separate transistors together with metal interconnects, *etc.* Detailed descriptions of the fabrication processes for Si can be found in Elliott [10] and for GaAs in Grant [2].

1.3 Dry Etching

A brief description of dry etching and the reasons for its increased use in IC fabrication was given in section 1.2.3.4.2. Since in this thesis, we are concerned with the energies that particles attain in dry etch systems, it is worthwhile spending some time discussing the main aspects of dry etching. Three main techniques in dry etching are widely used in the modern semiconductor industry. They range from the purely physical technique of sputtering, to the largely chemical mechanism of plasma etching, with reactive ion etching positioned between these two extremes.

1.3.1. Ion Beam or Sputter Etching

These are purely physical techniques in which the wafer sits on a pedestal inside an evacuated chamber at pressures of 10^{-2} - 10^{-5} Torr. *Ion beam etching* uses an ion gun to produce a beam of inert gas ions (usually Ar^+) which are accelerated towards the wafer through collimators. *Sputter etching* uses an RF discharge to produce the ions, which are then accelerated through the electrode sheath potential (see section 1.5.5) to strike the wafer surface. In both techniques, the ions have kinetic energies of several hundred eV and are highly directional. When they collide with the substrate atoms, momentum transfer occurs and the substrate atoms are knocked or *sputtered* from the surface. Since the ion direction is normal to the wafer surface, anisotropic etching is achieved and etch resolution is often very high [10]. Unfortunately though, this technique has many disadvantages:

- (i) Since the sputter yields of most semiconductor films and resists are very similar [26,27], selectivity is often very low, making end-points difficult to determine.
- (ii) High energy ions can heat the substrates to high temperatures, causing resists to flow or reticulate.
- (iii) Lattice damage can be severe [28].
- (iv) Redeposition of sputtered materials, especially on the sidewalls of etch wells [29] or even photoresist masks [30].
- (v) Implantation can occur at high ion energies.

It is the inherent disadvantage of (i) that makes ion beam and sputter etching difficult techniques to use to obtain the reproducible etching and stringent process controls necessary in the modern semiconductor industry.

1.3.2 Plasma Etching

In contrast to ion beam etching, *plasma etching* involves little physical sputtering, and is considered to be largely (although not completely) chemical in action. In some ways it resembles and gives similar results to wet etching. A glow discharge RF plasma is used to generate reactive species such as atoms, free radicals and ions from parent gases. The discharge is struck in a vacuum chamber containing the wafer, and the reactive species diffuse to the wafer surface where they react to form volatile compounds. These compounds then desorb from the surface and are pumped away.

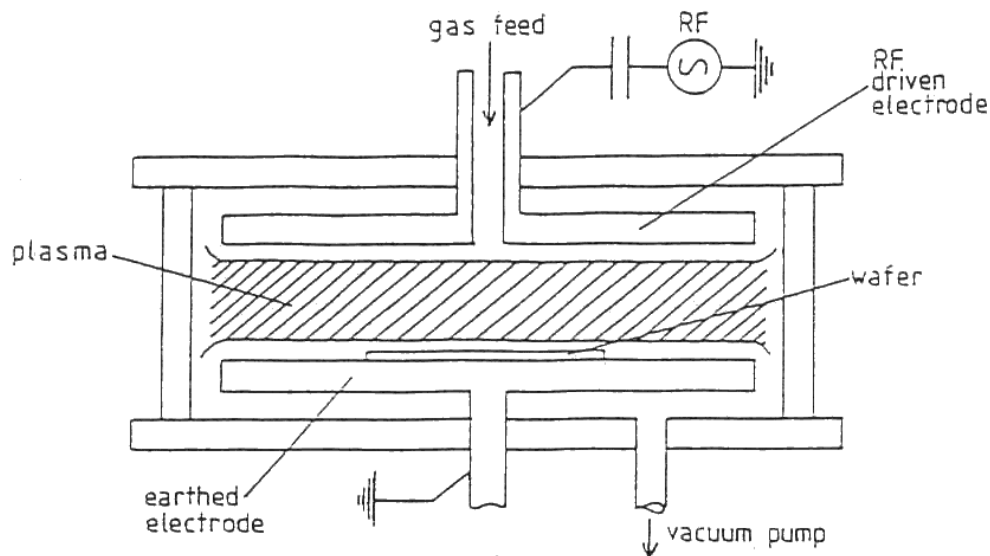


Fig.1.4. Diagram of a typical parallel plate reactor (after Thomas [30]).

A typical plasma etching reactor uses the planar or parallel-plate geometry illustrated in fig.1.4. This comprises two parallel electrodes of equal area. The wafer is placed upon the grounded electrode, and the other electrode is coupled to an RF generator via a capacitor. The

typical power level is a few W cm^{-2} at an RF frequency of between 50 kHz to 20 MHz. Typical pressures are 100-500 mTorr. The chemical 'soup' produced by the discharge interacts with the wafer surface.

The main advantage of using discharges is to produce highly reactive species from inert parent gases. For example CF_4 will not adsorb onto many surfaces [32,293], whereas F and CF_x ($x = 1-3$) produced in a CF_4 discharge have much higher sticking probabilities and so can readily adsorb and react with many surfaces [33].

In plasma etching the wafers can be subjected to bombardment from ions that have been accelerated through the sheath potential (see section 1.5.5). The impact of ions on the surface aids in etching and directly affects the degree of anisotropy. However, in a typical plasma etch reactor, the geometry is such that the sheath potential on the grounded electrode (anode) is only a few volts, and so the etching is predominantly isotropic (although under certain conditions anisotropic etching can be achieved [259]). Since plasma etching is closely related to wet etching, it shares many of its advantages (high selectivity, low damage) and disadvantages (tendency for isotropic etching, poor process control).

1.3.3 Reactive Ion Etching (RIE)

This combines the purely physical sputtering of ion beam etching with the chemical nature of plasma etching. Reactive ions produced in the discharge are accelerated onto the wafer surface at high energies, initiating both sputtering mechanisms and enhancing chemical reactions. Energetic neutral species produced by collisions with high energy ions also strike the wafer surface (see sections 6.10-6.12) to initiate etching mechanisms.

In RIE, the same planar reactor geometry is adopted, but the energy with which the ions strike the wafer is increased by placing the wafer on the powered electrode (cathode). The cathode is also much reduced in area, so making the electrode area ratio (cathode:anode) much smaller. This increases the *sheath potential* (see section 1.5.5) greatly by causing a *DC self-bias offset* to be developed which can be several hundred volts (see section 1.5.6). Higher ion energies are further encouraged by reducing the operating pressures of typical RIE systems to <100 mTorr. A typical RIE reactor is shown in fig.1.5.

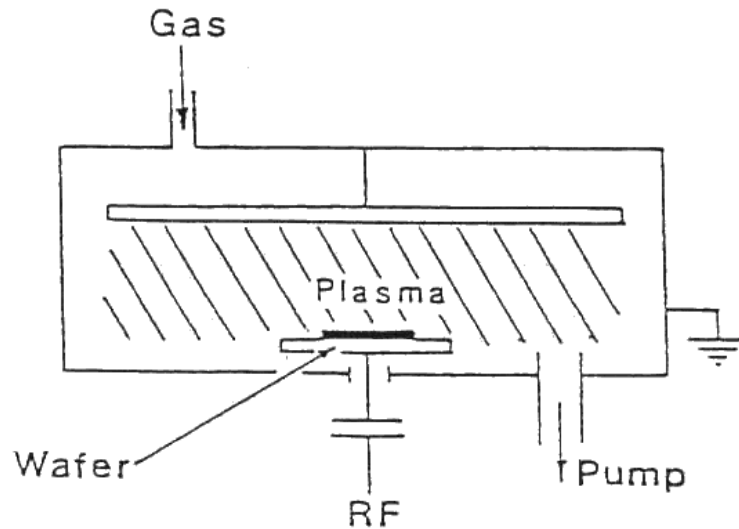


Fig.1.5. Diagram of a basic RIE reactor (after Hydes [31]).

Since RIE processing combines the physical aspects of ion beam etching with the chemical nature of plasma etching, it is possible to develop processes which have all the benefits of ion beam etching (fast etch rates, anisotropic etching, *etc.*) with those of chemical etching (high selectivity, low damage, *etc.*), without the disadvantages of either. This of course, is the ideal case, and obtaining such process conditions is seldom easy. Some typical RIE processing problems are discussed in section 1.3.4.1.

RIE is now the dominant technique for pattern transfer in the semiconductor industry and is used in almost every etch step in the fabrication line, from the defining of the polySi gate and the opening of shaped contact holes [10], to the delineation of complex multi-level interconnects [30]. However, for such a widely used technique, remarkably little is known about the fundamental processes controlling etching, especially the role that energetic ions perform. This, therefore, has been the motivation behind the work contained in this thesis.

1.3.4 Etch Processes

A brief discussion of some of the typical processes used in the RIE of common materials will be given in section 1.3.4.2. Before this is done, however, a brief outline of some of the common problems encountered when developing RIE processes is presented. It must be pointed out that this list is by no means exhaustive; many more problems can arise with an etch process than can be mentioned here, so only the main effects are discussed. An example of each of the following phenomena is shown in fig.1.6.

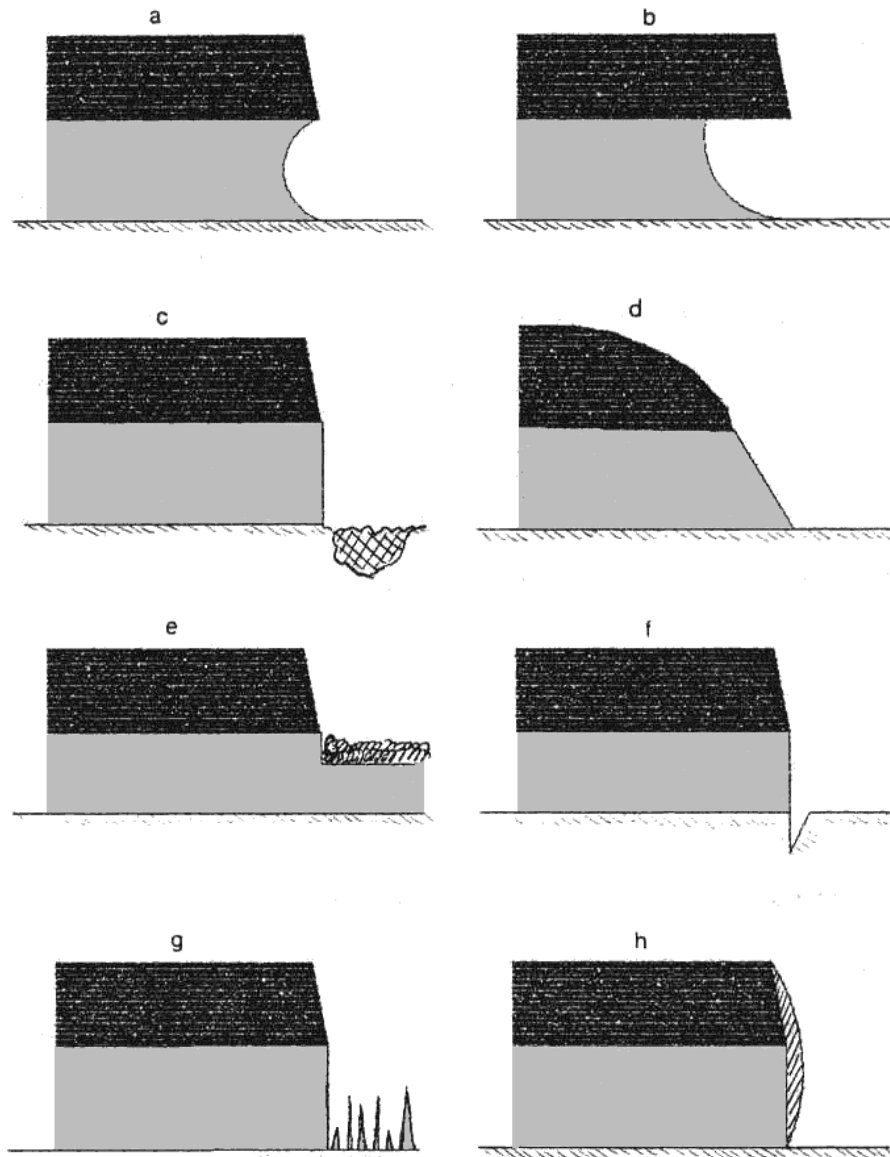


Fig.1.6. Typical problems that occur with etch processes and their resulting sidewall profiles. The resist is shown shaded.

1.3.4.1 Common Problems Observed with RIE Etch Processes

- (a) **Re-entrant profiles** [9]: If the process conditions are not carefully controlled (particularly the gas pressure), collisional processes can scatter the ions passing through the sheath into non-vertical trajectories. This can lead to re-entrant profiles and linewidth loss [86] as is demonstrated in section 8.4.
- (b) **Isotropic Etching** [9]: Certain processes are less dependant upon ion bombardment

to initiate etch mechanisms. Free radicals in the plasma etch some materials rapidly. A combination of these two effects can lead to isotropic etching, even in an RIE environment. The result can be an undercut profile, in a similar fashion to that seen for wet etching. A typical example often occurs when etching Al with Cl₂ plasmas.

- (c) **Lattice Damage** [9]: High energy ion bombardment of the semiconductor surface can induce defects into the crystal lattice. These defects often only appear later when the finished device is tested and exhibits substandard performance. Damage can take many forms; dislocations and rearrangement of lattice atoms, implantation of reactive or unreactive plasma species and ionisation of lattice atoms, amongst many others.
- (d) **Resist Damage** [10]: The photoresist mask is also subjected to the hostile environment of the etching plasma and may be seriously eroded during the etch. This can lead to significant linewidth loss for small features. If ion bombardment is excessive, or the wafer temperature becomes too high during the etch, the resist can melt, wrinkle or reticulate in an unpredictable and uncontrollable way. Some RIE processes however, apparently require a certain degree of resist erosion in order to provide the carbonaceous species that are thought to be a mechanism for sidewall passivation [183].
- (e) **Polymer Deposition** [10]: Most RIE plasmas use halogenated carbon compounds as etchant gases. One of the main problems associated with carbon-containing gases is the formation of long-chain polymeric compounds, which then deposit upon the wafer surface. This can seriously degrade etching performance and in certain cases inhibit etching totally.
- (f) **Trenching** [10,89]: If ion bombardment is too vigorous, ions can reflect off the resist or etch sidewall and produce a V-shaped trench close to the base of a feature. This can seriously affect device performance.
- (g) **Micromasking** [39]: Submicron particles on the wafer surface can act as micromasks, protecting the underlying surface in a similar fashion to the resist. Highly directional etch processes then produce spikes in the layer. This is often termed *black silicon* [40]. The problem is usually overcome by a pre-etch clean step, or by using a higher pressure etch process whereby the less-directional ions can undercut the spikes leaving a smooth surface.
- (h) **Redeposition of Sputtered Material**: RIE is often used to etch materials that cannot be removed easily by chemical means (*e.g.* copper in AlCu alloys). This is achieved by effectively sputtering these materials from the surface in high power RIE etches. Since these materials are not chemically combined into a volatile compound, they often just redeposit elsewhere on the wafer (possibly forming micromasks). If the redeposition is back onto the substrate surface, this can inhibit etching. Involatile material can also deposit on the sidewall forming a passivation layer [183], so aiding

anisotropy, or even onto the resist protecting it from erosion [30].

1.3.4.2 RIE Processes for Specific Materials

The basic requirement for an RIE process is to create a volatile chemical compound containing atoms from the substrate surface. This volatile compound is then pumped away exposing a fresh surface beneath. A brief outline of the major etch processes used in the modern semiconductor industry is given below for different materials.

1.3.4.2.1 Silicon and Polysilicon

Si can be etched by halogen-containing gas plasmas, since the reaction products (SiF_4 , SiCl_4 , *etc.*) are volatile. The normal process gases used are CF_4 , SF_6 , Cl_2 , and CCl_4 , since these are readily available and relatively safe to handle. It has been found that additions of up to 8% of O_2 into the gas mixture increase etch rates considerably, due mainly to surface polymer removal. The underlying layer is often SiO_2 , consequently selectivity is not usually a problem since Si-O bonds are stronger than Si-Si bonds [160]. Therefore, a process that etches Si easily, will not be as effective in etching SiO_2 . Greater selectivity can be achieved by using Cl-based process gases, but at the risk of producing black Si effects [39,40].

1.3.4.2.2 Silicon Dioxide

SiO_2 provides a challenge to etch process engineers, particularly when selectivity is required to an underlying Si layer. Often polymer-producing plasmas are used to deliberately deposit controlled amounts of fluorocarbon polymers onto the wafer surface. The gases used typically have a high carbon:fluorine ratio promoting the growth of long-chain polymers [46,47]. Examples are C_2F_6 or CF_4/H_2 mixtures, where the H_2 scavenges F atoms increasing the effective C:F ratio. The polymer is deposited on all the wafer surfaces, but since SiO_2 contains a 'built-in' supply of O_2 , any etching releases O_2 which reacts with and removes the polymer. Consequently, the oxide etch rate is not significantly affected by the polymer layer. Si, however, has no supply of O_2 with which to remove the polymer, consequently the polymer layer builds up, greatly inhibiting the Si etch rate.

The process engineer must control the plasma conditions within strict limits. If polymer deposition is too rapid, the oxide stops etching also, but if too little polymer is deposited, the Si etch rate increases rapidly and selectivity is destroyed. As might be expected from such a 'knife-edge' process, oxide etches are very difficult to control and often give poor day-to-day uniformity. Oxide etch reactors become 'dirty' due to the polymer coating on most surfaces and have to be cleaned regularly.

1.3.4.2.3 Aluminium

The metal interconnects used to join transistors together are usually made from Al, sometimes containing up to 1.5% of Si to prevent dissolution of Si into the Al [48], and occasionally up to 4% Cu to aid electrical properties (such as decreasing *electromigration* [49]). Since Al fluorides are relatively involatile, Al can only be etched in Cl-based processes, with AlCl₃ being the etch product. Unfortunately, AlCl₃ reacts with water vapour to produce highly corrosive HCl, which rapidly corrodes the delicate metal structures on the wafer. Metal etch reactors are designed therefore to prevent water vapour entering the chamber, either by use of multiple load-locks, very low base pressures, water-scavenging process gases (*e.g.* BCl₃), or combinations of any of these. Typical process gases [9,10] are; CCl₄, SiCl₄, BCl₃, and Cl₂, which are usually diluted with other gases. A major problem with Al etching is that Cl₂ etches Al spontaneously (*i.e.* without the need for a plasma), leading to isotropic profiles. This is often overcome by introducing a carbon-containing gas to produce a polymer that deposits onto the sidewall forming a passivating layer. Alternatively F-containing species (*e.g.* 5% CF₄) are added to preferentially fluorinate the sidewall, preventing undercut. Occasionally a sidewall passivation layer is produced by deliberately eroding the resist and allowing the polymer-forming carbon compounds to enter the plasma. This is often done by adding noble gases such as Ar or He which can sputter particles from the resist.

Another problem observed when etching Al is the induction period associated with the removal of the native oxide present on the metal surface. The etch rate of this oxide is much less than that of the metal, consequently even small differences in the thickness of the oxide in different regions of the wafer lead to poor across-wafer etch uniformity. BCl₃ or SiCl₄ are often added to the process gas mixture to act as reducing agents, allowing the oxide layer to be removed quickly.

1.3.4.2.4 Multi-layered Structures

Often a process has to etch through more than one layer sequentially. Typically examples are *polycide gate structures* [180], or *multi-layered metal structures* [30]. These often necessitate multi-stage etch processes with changes of chemistry for each layer and individual end-point determination for each interface. An example of just how complex these etch processes can become is given by May and Spiers [30] who demonstrated an anisotropic etch process for a three-layered sandwich of TiW/AlSi/TiW that remained selective to the underlying oxide layer.

1.3.4.2.5 Gallium Arsenide and Indium Phosphide

The major requirements for GaAs etch processes are fast etch rates without leaving residues, and selectivity to the underlying AlGaAs. Most processes gases used to etch Si do not meet the stringent requirements for GaAs etching, and new processes have had to be developed for most III-V compounds. The processes gases used are typically a mixture of both F chemistry (for fast etch rates) and Cl chemistry (for selectivity). Another problem is that due to the presence of a thin oxide film on the surface of most III-V materials, etch process reproducibility is often poor. Smolinsky *et al* [41] found that gases such as Cl₂ or COCl₂ did not etch this native oxide and HCl etched it only slowly. Many other likely etchants form polymers that prevent etching. One gas

that is often used to etch GaAs and its oxide is CF_2Cl_2 , sometimes in the presence of He [42] for greater selectivity to AlGaAs. CFCl_3 has also been successfully employed to etch GaAs [43].

Like GaAs, InP can be etched in CF_2Cl_2 plasmas [44], but it has been shown [45] that the relatively unreactive gas mixture of CH_4/H_2 is a very good etchant for this material in the presence of an RF discharge. It is believed that the H_2 reacts with the P to form PH_3 which is pumped away, and then the In is removed by a sputtering mechanism. Evidence for this mechanism comes from the fact that emission from In atoms has recently been observed when etching InP in a CH_4/H_2 plasma [260].

A review of etchants used to etch GaAs, InP, and other III-V materials is given by Wade [43].

1.3.4.2.6 Miscellaneous Materials

There are many other materials that often require etching. In the semiconductor industry these include: Si_3N_4 , WSi_2 , W, Ti, AlSiCu, polyimide, and borophosphosilicate glasses, along with novel superconducting materials, such as Nb, YBaCuO, and BiSrCaCuO. Each of these materials has a dry etch process optimised for its own characteristics. The processes have almost always been developed by empirical methods.

1.3.4.3 The Effect of Plasma Conditions Upon Etching

An RF discharge is a very complex system with many parameters which all interact together in subtle ways to produce the final etch process. The factors which influence the performance of a process are many and varied and are often inter-related. Consequently it is almost impossible to make a definitive statement about the effect of one particular plasma parameter upon the etch performance. When developing a new process, an engineer usually performs a series of etch-trials on a grid basis, to try and find, and then narrow down the process window that has the optimum performance for his requirement. This procedure can often be a matter of trial-and-error, and a good process can sometimes be achieved more by luck than judgement. However there are a few broad principles which are generally true. These 'rules-of-thumb' are outlined below for the main adjustable plasma parameters.

1.3.4.3.1 RF Power

RF power supplied to the plasma is typically between 50 and 300 W for single-wafer machines. Its magnitude determines the amount of energy delivered to the various species within the plasma. Experiments show that power is proportional to the RF voltage, V_0 (see section 1.5.2) applied to the lower electrode, and hence determines the sheath potential (see section 1.5.5). This direct proportionality between power and V_0 holds for the typical power levels used in RIE processes, but at very low powers (< 30 W) power becomes proportional to V_0^2 . This result has been experimentally confirmed on the present apparatus (the Minstrel etcher, see section 2.4) and other commercially available reactors [289].

Increasing the RF power has a number of major effects upon the plasma. The electron and ion temperatures (see section 1.5.3) are increased, so providing more energy for bond-breaking collisions and gas-phase reactions. An increase in electronic excitation reactions (section 1.5.9) is exhibited by the plasma becoming brighter. Also, with higher powers there is an increased chance that long-chained molecules will be broken apart by collisions with energetic electrons, leading to a decrease in polymer formation. As the sheath potential increases, ions strike the electrode with greater energy, so increasing the etch rate and the surface damage. Also, the wafer tends to reach a higher temperature due to more energy being deposited onto its surface by the ions. These two effects often lead to resist erosion problems with high power etch processes. RIE reactors therefore make provision for cooling of the walls and electrodes (see section 1.3.4.3.5). High energy ions are not so easily deflected by collisions in the sheath, and are consequently more directional than lower energy ions. This can cause trenching, back sputtering and micromasking effects. High power processes often leave rough surfaces due to micromasking effects, and occasionally cause lattice damage that affects device performance. Too low a power however, results in unacceptably slow etch rates, possible polymer deposition problems and reduced anisotropy.

1.3.4.3.2 Frequency

Most RIE reactors use the F.C.C. (US Federal Communications Commission) standard frequency of 13.56 MHz, which was originally allocated for etching purposes in a region of the RF wavebands not used for communications. Only recently have workers started looking at the effect of frequency upon etch characteristics [49,90]. At lower frequencies (~100 kHz), the average energy of the ions bombarding the substrate is much higher (see section 5.2.5). This leads to increases in etch rate and anisotropy, but can enhance the disadvantageous effects of resist damage, micromasking and poor selectivity.

1.3.4.3.3 Gas Pressure

This is one of the most crucial plasma parameters, and increasing pressure generally has the opposite effect to that of RF power. An increase in pressure at constant power level leads to a decrease in the average amount of energy for each species in the gas phase. Consequently, the rates of chemical reactions in the bulk of the plasma are reduced and the plasma becomes dimmer. As the pressure increases, electrons no longer possess enough energy to break C-C bonds and so the concentration of large molecules (such as polymeric species) can become significant. Ion bombardment of the wafer surface is also increasingly modified by sheath collisions, lowering the average energy of ion impact, and so lowering the etch rates for reactions that require ion-assisted desorption of etch products. However, since there are now more reactive neutral species within the plasma, an increase in pressure often leads to an increase in chemical (isotropic) etch rate, with its resulting mask undercut [86]. This increase in etch rate often continues until a pressure is reached where the chemical species have so little energy that they can no longer overcome the activation energy required to undergo surface reactions. At this point, further increases in pressure result in a drop in etch rate. This is illustrated in fig.1.7 for a

GaAs etch process using CF_2Cl_2 .

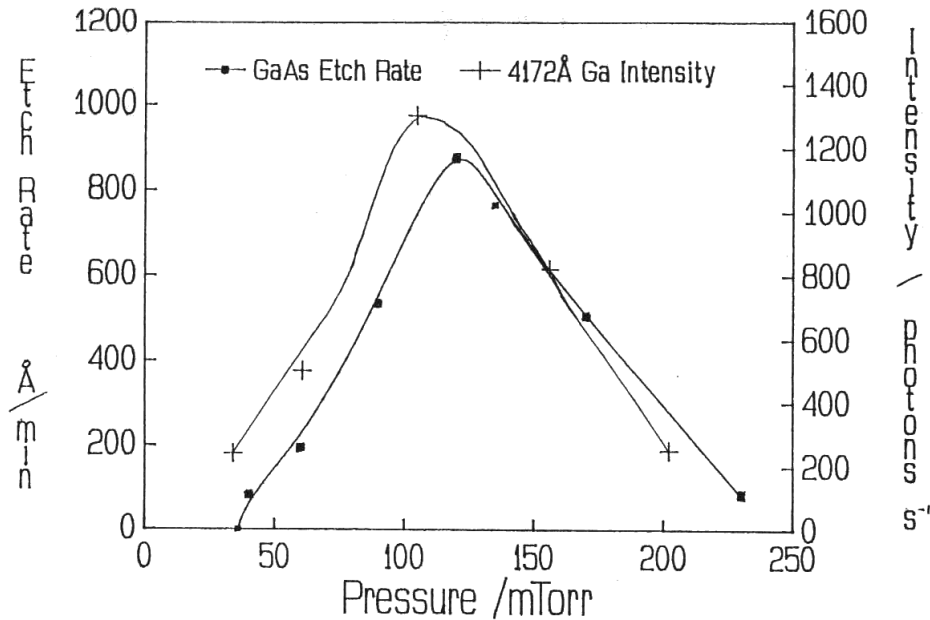


Fig.1.7. Etch rate of GaAs and optical emission intensity of the 4172 Å Ga line as function of pressure for the standard CF_2Cl_2 etch process conditions described in section 2.7.

The *residence time* in a plasma chamber is defined as the mean time spent inside the chamber by a gas molecule [47]. For a rotary pump the pump rate is generally constant over the range of pressure usually used for RIE processes. Consequently, the residence time is directly proportional to pressure and inversely proportional to gas flow rate. The residence time can vary from a few milliseconds to a few tens of seconds depending on the flow and pressure. At low pressures the residence time is so small that gas molecules are often swept out of the chamber before they have had a chance to strike the substrate surface and react. Conversely, at higher pressure, molecules spend much longer times in the chamber, diffusing to all the surfaces where they react. Consequently, we find that ion-enhanced reactions dominate at low pressures, and diffusion-based chemical reactions at higher pressures. As the pressure is raised from a few mTorr to >100 mTorr, etch profiles start off vertical and anisotropic with rough surfaces, and gradually become re-entrant and isotropic with smoother surfaces. Simulation of these effects form the basis of section 8.4.

1.3.4.3.4 Gas Flow Rate

In most RIE processes the gas flow rate is a much less important parameter. It is occasionally used in conjunction with pressure to control the uniformity of etching across a wafer. The main contribution of flow rate to the plasma process involves the residence time of the plasma species, although flows are generally kept in a regime where there is always a plentiful supply of reactant to prevent reactant-limited etching occurring. When the etch process

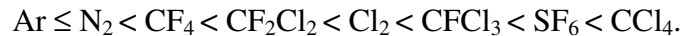
becomes reactant-limited, loading effects can occur and across wafer uniformity can be degraded. Typical flow rates are a few standard cubic centimetres per minute (sccm). The effects of flow upon plasma conditions for some etch processes are discussed by Chapman [47].

1.3.4.3.5 Wafer Temperature

Energetic ion bombardment of the wafer can cause it to heat up significantly. Most RIE chambers have water or oil-cooled electrodes to minimise these effects and maintain the wafer at a constant temperature. Some reactors even have the back of the wafer in direct thermal contact with He gas to ensure uniform heat removal from the wafer [182]. If the wafer temperature gets too high, resist melting may occur, or 'hot-spots' may develop which allow increased localised etch rates, leading to poor across-wafer uniformity. Certain processes require cool etching to encourage polymer deposition (*e.g.* SiO₂ etching), whilst others need to desorb volatile (and potentially corrosive) etch products, and so keep the wafer at elevated temperatures of up to 80°C (*e.g.* Al etch processes).

1.3.4.3.6 Electronegative and Electropositive Gas Plasmas

Plasmas are usually characterised into two different types depending upon the electron affinity of the process gases used. Table 1.1 gives a list of common etch gases with their integrated total electron attachment cross sections and attachment rate constants. From this table the process gases can be arranged in order of increasing electronegativity:



We shall look at each type of plasma in turn.

Table 1.1. Total electron attachment cross sections (*EACS*) for typical process gases [149].
Cross sections are integrated between 0.04 and 2.5 eV, *i.e.*:

$$EACS = \int_{0.04}^{2.5\text{eV}} \sigma(E).dE$$

The table also gives the attachment rate constant, k_{th} for thermal (300 K) electrons [149],
* estimated from data in ref.[150].

Process Gas	<i>EACS</i> / $10^{-16} \text{ cm}^2 \text{ eV}$	k_{th} / $10^{-8} \text{ cm}^3 \text{ s}^{-1}$
CCl ₄	24.9	23.7
SF ₆	11.1	24.9
CFCl ₃	6.4	1.2
* Cl ₂	~3.0	~20.0
CF ₂ Cl ₂	0.66	0.012
CF ₄	<0.1	<10 ⁻⁴
N ₂	0.0	0.0
Ar	0.0	0.0

(a) **Electropositive (EP) plasmas:** These are discharges consisting mainly of species that do not form negative ions easily. Examples of EP gases are all the noble gases such as Ar, He, and some unreactive gases such as N₂. In these plasmas, the number of positive ions is almost exactly equal to the number of electrons, although both are still very much smaller than the number of neutrals. The relatively large abundance of electrons enables EP plasmas to be easily initiated and sustained at very low power levels. Due to the high mobilities of electrons, they can travel to all parts of the plasma region. Consequently EP plasmas tend to be very uniform and stable. Typical electron temperatures for these plasmas are around 1-2 eV (see section 1.5.3).

(b) **Electronegative (EN) plasmas:** By contrast, EN plasmas contain a significant number of species which have a positive electron affinity and cross-section for electron attachment. These plasmas include most of the fluoro- or chlorocarbon process gases used in semiconductor etching processes. In these cases, the number of free electrons is significantly reduced as a result of capture by EN species to form negative ions. A typical reaction is shown below for CCl₄, which has an extremely large cross section for electron capture.



In CCl₄ plasmas, the number of electrons can be up to 100 times less than the number of positive ions, with overall charge neutrality being maintained through large numbers of negative ions [82]. The relative lack of electrons in EN plasmas inhibits energy transfer into the discharge from the applied electric field (see section 7.2). Consequently, EN plasmas require higher powers to sustain them and are often difficult to initiate. Therefore EN plasmas are often non-uniform and unstable. The electron temperature is also much higher than that seen in an EP

plasma for two main reasons: (i) the low energy electrons are removed by attachment reactions (since they have a larger cross-section than faster electrons), leaving only the higher energy ones, and (ii) the energy put into the plasma by the electric field is distributed to fewer electrons, consequently the average energy per electron increases. Typical electron temperatures for EN plasmas are 5-10 eV [81,82]. The electron energy distribution for an EP gas (N_2) and an EN gas (CCl_4) have been measured [82] by Langmuir probe techniques (see section 1.4.5). A comparison of these is seen in fig.1.8.

(c) **Intermediate plasmas:** Some process gases exhibit small (but non-zero) electron attachment cross-sections. Consequently, these plasmas form some negative ions, but the number of electrons is still greater than the number of negative ions, so these plasmas cannot be called true EN plasmas. Examples of these intermediate plasmas are CH_4 , H_2 , O_2 and to some extent CF_4 . The latter does produce a large number of negative ions, but not as many as the true EN gases such as CCl_4 *etc.* As might be expected, intermediate plasmas exhibit features somewhere between the extremes shown by EP and EN plasmas.

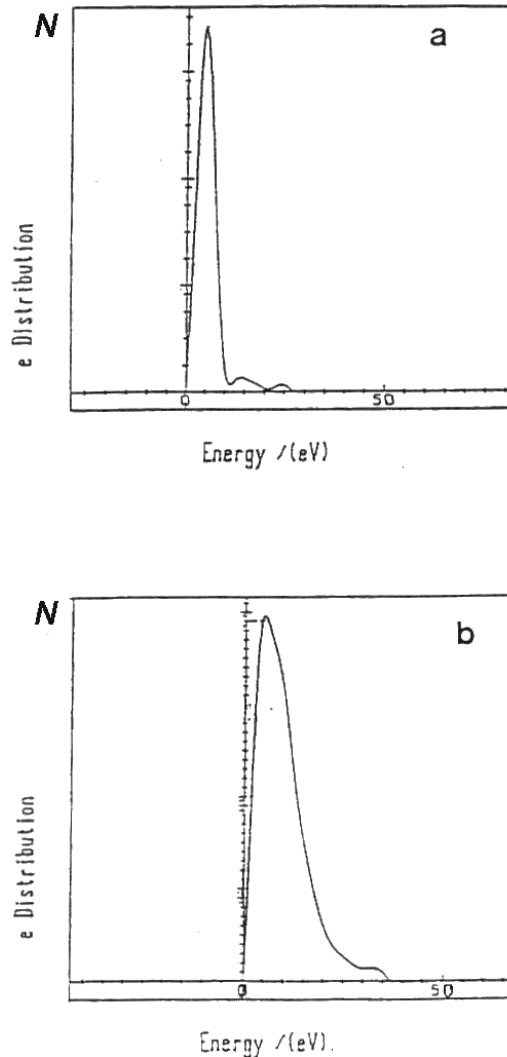


Fig. 1.8. Electron energy distributions obtained by an electrostatic RF-compensated Langmuir probe technique [82], for (a) N_2 and (b) CCl_4 , plasmas. The N_2 distribution is concentrated at low energies whereas the CCl_4 distribution shows a much higher overall energy with a tail extending out to about 37 eV. The absolute number of electrons in the CCl_4 plasma was measured to be 100 times less than in the N_2 plasma.

1.3.4.3.7 The Role of Gas Composition

The main gas in the process is usually chosen for its ability to etch the required material, but then other gases are often added to optimise the process. Some of the common additives are now discussed, along with the reasons for adding them to the process and their effects upon the plasma.

- (i) O_2 is often added to fluoro- or chlorocarbon plasmas. This generally increases the etch rate of most materials for two main reasons: (a) it prevents polymer formation on the wafer surface by oxidising carbon, and (b) CO or CO_2 formed by reaction of O_2 with the parent gas

liberates extra halogen atoms [47].

- (ii) H_2 is occasionally added to scavenge F atoms and thus increase the C:F ratio in oxide etch processes. This encourages polymer formation and hence increases the selectivity of oxide to Si (see section 1.3.4.2.2).
- (iii) BCl_3 or SiCl_4 are often used as main process gases, or as additives to Cl_2 -based processes. Their main functions are to (a) scavenge water vapour to prevent corrosion of metal features by HCl (see section 1.3.4.2.3) and (b) to act as reducing agents, removing the native oxide on metal surfaces, thus eliminating the induction period and allowing a more uniform etch process.
- (iv) Ar, He and N_2 are very EP gases which ionise relatively easily. They are often added to EN plasmas to provide a source of electrons to these electron-depleted discharges. This stabilises the plasma, increases the uniformity of etching and generally counteracts many of the unfortunate side-effects that F- or Cl-based plasmas exhibit.

1.4 Plasma Diagnostics

The microelectronics industry has reached a point where the technology leads the science, especially in the field of RIE etching. Indeed, plasma process engineering is often described as more of an art than a science. It is this lack of knowledge about basic plasma processes that has been the driving force behind plasma diagnostics. It is only by understanding processes on a more fundamental basis that etch mechanisms can be evaluated. This should eventually lead to better etch processes, improved reactor design and faster process development, with less dependence upon the empirical ‘rules-of-thumb’ described in section 1.3.4.4.

A plasma is an extremely complex system and a complete characterisation of all the processes occurring within it would be virtually impossible. Indeed, this would require knowledge of the chemical identity of all the neutrals and charged particles, along with their density and energy distributions at all points in the reactor. We would also need to know the way in which these particles interact with the electrodes, the substrate and each other.

Plasma diagnostic techniques have been developed to study some of these phenomena. The aim is to further the understanding of plasmas in order to monitor and improve the performance of existing processes and to develop new ones. Coburn [50] has recently reviewed plasma diagnostic techniques in detail, so only a brief account of the major techniques will be given here.

1.4.1 Etch Rate Measurement

This is one of the simplest methods of obtaining information about the plasma. The amount of material removed during an etch process is usually measured by dragging a sensitive stylus across the wafer surface. The stylus is connected to instrumentation that records its vertical position. As the stylus passes over a raised etched feature, the stylus rises and the height

increase recorded. Commercially available *profilometers* of this type (such as *Tallystep* or *Dektak*) are capable of measuring step heights of down to 10 Å.

If a profilometer is not available, etch rates can be determined by the *weight-loss method*. If the wafer is weighed before and after etching, and has a known exposed surface area, the etch rate is given by:

$$\text{Etch rate (Å min}^{-1}\text{)} = \text{Weight loss (10}^{-8}\text{ g min}^{-1}\text{)} / \text{Density (g cm}^{-3}\text{)} \times \text{Area (cm}^2\text{)} \quad (1.4.1)$$

This equation assumes that etching is uniform across a wafer surface. A balance accurate to ± 0.1 mg is generally required to measure the weight loss associated with etching away about 1 μm of material.

1.4.2 Scanning Electron Microscopy (SEM)

An SEM is a microscope that rasters a beam of electrons across a sample enclosed in a vacuum chamber [67]. Resolutions of down to 100 nm can be obtained and so SEMs are especially useful for examining etch profiles [30], etch-induced damage, surface contamination [68-71] and obtaining accurate etch rates. Their simplicity of use has led to SEMs being widely used by process engineers to develop new etch processes. Detailed descriptions of SEM constructions and operation can be found in ref.[67].

1.4.3 Surface Analytical Techniques

After etching, the surface of a wafer can be examined to identify the chemical composition of the upper atomic layers. There are many techniques available to probe the substrate surface, such as SIMS, RBS, AES, UPS and XPS. A description of these can be found in most modern textbooks on surface science [51,261]. These techniques nearly all rely on bombarding the surface with a flux of particles (ions, electrons or photons) of known energy, and observing the resulting emission of secondary particles ejected from the surface. Measurement of the type or energy of these secondary particles yields the chemical composition of the substrate. An example is *X-ray Photoelectron Spectroscopy* (XPS), where the surface is exposed to a beam of monoenergetic X-rays. The energy distribution of photoelectrons emitted from the surface shows characteristic peaks corresponding to the electron binding energies of the particular elements present in the surface. Composition depth-profiling can be constructed by combining XPS measurements with ion beam milling [261]. Elemental maps can be obtained by combining AES with SEM in the *Scanning Auger Microprobe*.

1.4.4 Mass Spectroscopy

Mass spectroscopy has been used as a diagnostic tool to study many plasma etch processes [52-57]. The most commonly used instruments are *quadrupole mass spectrometers* due to their

convenience and flexibility. Two basic approaches have been adopted when using mass spectroscopy to study plasma systems. The first is to place the analyser downstream from the plasma, so that only the neutral effluent gas mixture is sampled. The trouble with this *residual gas analysis* is that the results obtained often bear little or no relation to the composition of the species in the reaction chamber. Most species will have taken part in gas-phase reactions on their passage through the lengthy pumping system from the chamber to the analyser, and their nature may have been altered significantly before they are detected. To get around this problem, direct sampling techniques have been developed. In these, the analyser is positioned as close as possible to the plasma, while ensuring that the plasma is disturbed as little as possible. Techniques used include positioning the entire analyser within the discharge itself [58-60], or allowing plasma species to effuse directly into the analyser through holes drilled in the electrodes [61-65] or chamber walls [66]. Alternatively, the analyser is connected to the plasma reactor via a thin glass capillary probe [31,53]. Techniques such as these can greatly aid in the evaluation of some of the complex chemical reaction pathways occurring in the plasma bulk. Mass spectrometers have also been used successfully to measure end-points and provide real-time etch process monitoring [267].

1.4.5 Electrostatic (Langmuir) Probes

Electrical probe measurements consist, in the simplest case, of inserting a wire into the plasma to measure the potential at different locations. This yields information about ion and electron temperatures and densities, along with the plasma potential [81,82] (see sections 1.5.3-1.5.6). These probe techniques are reviewed by Kushner [83], Clements [84] and Swift and Schwar [85].

One of the main problems with Langmuir probe measurements is interference caused by RF modulation of the signal by the oscillating plasma potentials. Attempts to overcome this problem have included feeding a compensating RF modulation from the generator directly to the probe tip, in the hope that the two oscillations will cancel out [81,82]. However, this assumes the plasma potential can be represented as a sinusoidal variation, which is untrue [148]. This fact, along with the problems of probe tips etching away, make the interpretation of Langmuir probe measurements in corrosive gas RIE plasmas subject to a good deal of uncertainty. The presence of negative ions within the plasma can also affect the reliability of probe measurements [82,268].

1.4.6 Optical Emission Spectroscopy (OES)

This has been the most popular diagnostic technique used to date, due to its relative simplicity and non-invasive nature. Numerous workers have used OES to examine discharges [87-95], both to investigate the chemistry occurring within the plasma and to aid in the detection of end-points. Most RIE etchers bear a quartz window which allows the emission from electronically excited species within the plasma to be studied. The light emitted from these species as they undergo electronic transitions passes through the window into a spectrometer where it is dispersed and detected by a photomultiplier. The fluorescing species can be identified from the wavelength of the bands (for molecules) or lines (for atoms and ions) present in the

spectrum. Certain emission lines can be used to monitor the progression of the etch process and are often used for end-point determination. For example, F atom emission has been used to study Si etching in CF₄ plasmas[31].

1.4.6.1 Actinometry

One of the main drawbacks with OES is that the intensity of an emission line cannot be taken as a direct measure of the ground state concentration of the emitting species [99]. To overcome this, a technique called *actinometry* has been developed [96-100]. This involves admitting a small known amount of a tracer gas (*e.g.* Ar) to the main process gas (*e.g.* CF₄). The emission from both species is monitored and the concentration of F can then be calculated from the ratio of the intensities of a F line to that of an Ar line [43]. This technique has proved to be successful for F atom measurements [99,100], but does not work for Cl [101,102]. Use of N₂ as an actinometer to normalise CCl emission also fails [103]. The conclusion of those workers looking at the actinometry of Cl-based systems was that actinometry is likely to be invalid if used to measure radical concentrations derived from the decomposition of parent molecules (see section 4.7.7).

1.4.7 Miscellaneous Plasma Diagnostic Methods

There are numerous other plasma diagnostic techniques which have been used to examine plasma processes. Techniques such as *Fabry Perot Interferometry* and *ion energy analysis* form a major part of the work described in later chapters of this thesis, therefore a detailed introduction to these two diagnostic methods is given in sections 1.6 and 1.7, respectively. Other techniques need only be mentioned briefly. These include:

- a) **Infrared and Fourier Transform Infrared Spectroscopy** are occasionally used to study plasma-deposited films [68], or in the identification of surface contaminants [69]. They have also been used to examine condensed effluent gas [76]. Use of a tuneable infrared diode laser has recently allowed absorption spectroscopy of CH₄ plasmas to be performed [266].
- b) **Transmission Electron Microscopy (TEM)** gives resolution of a few Å when studying thin films (100 nm) of materials. It is often used to study defects in the crystalline lattice [67].
- c) **Macroscopic Discharge Parameters** such as pressure [70], DC bias [71] or substrate temperature [72] can sometimes be used for end-point detection, or to gain insights into reaction mechanisms.
- d) **Laser Induced Fluorescence (LIF)** is used to probe the concentration of ground state species in the plasma in a non-invasive fashion [73-75]. Hancock [262] has used LIF to study the validity of actinometry for CF₄/O₂ plasmas with increasing partial pressures of O₂. He has also used time-resolved LIF to study the loss rates of reactive radicals from surfaces.
- e) **Titration** has been used to study F atom concentrations using Cl₂ gas [76,77].

- f) **Chemiluminescence** monitoring downstream has been linked to Si etch rate [78,79].
- g) **Ellipsometry** is a branch of reflectance spectroscopy in which the change of polarisation state of a laser beam which is reflected from a substrate surface is measured. It can be used as a real-time *in-situ* monitor of the wafer being processed, giving information on etch rates, end-points, presence of residual layers, surface roughness and polymer deposition [80,263-265].

1.5 The Physics of Discharges

We now turn to the basic physics of the discharge. We shall pick out only those parts which are relevant to the present work, only touching briefly upon other aspects of plasma physics. A comprehensive account of many of the important plasma phenomena is given by Chapman [47].

The low pressure plasmas dealt with in this thesis consist of a partially ionised gas containing atoms, molecules, electrons, positive and negative ions and photons. The plasma has overall charge neutrality, so that the number of positive and negative particles are, on average, equal. The degree of ionisation is typically 10^{-4} so the plasma is composed mainly of neutral molecules and radicals [47]. The density of charged particles is typically 10^{10} - 10^{11} cm^{-3} although this value will vary depending upon the exact plasma conditions, especially the RF power. The physical and chemical processes maintaining the plasma result in the system reaching a non-equilibrium steady state, which is determined by the rates of production and loss of active species.

1.5.1 Initiation and Maintenance of the Discharge

The discharge is started by an electron that originates from either (a) photoionisation of a neutral species by cosmic rays or background radiation, or (b) field emission caused by strong electric fields around a sharp point at the electrode surface. The applied electric field will accelerate the electron, causing it to undergo scattering collisions with gas molecules. Eventually the electron will possess enough kinetic energy to ionise a gas molecule through an inelastic collision. This will release another electron, and so a cascade mechanism is rapidly set up whereby other gas molecules are ionised in subsequent collisions.

To sustain the plasma, electrons must be generated at a rate which is large enough to offset the loss of electrons to the chamber walls, recombination with positive ions and/or electron attachment reactions. The main mechanism thought to be responsible for generating sufficient electrons to sustain the plasma is secondary electron emission from electrode surfaces [142]. This is caused by either metastable atom, electron, or positive ion bombardment of the electrode (see section 7.3.1). The electrons liberated are accelerated back through the large sheath potentials into the bulk of the plasma, where they may undergo ionising collisions.

For high frequency plasmas (>1 MHz), another sustaining mechanism can occur [142]. Field fluctuation in the body of the plasma accelerates electrons, which then undergo collisions with gas molecules. Most of these electrons will not have sufficient energy to cause ionising reactions. But electrons in the high energy tail of the distribution can have energies of tens of eV, and so these will be able to produce ionisation. However these high energy electrons will only amount to a few percent of the total electron population.

1.5.2 DC and RF Discharges

Radio frequency (RF) discharges are preferred over DC-driven discharges in plasma etching systems for two main reasons: (a) the energy transfer to the discharge is more efficient at RF frequencies, and (b) RF-driven discharges allow insulators to be etched, which is not possible in DC discharges due to substrate charging effects. Consequently nearly all commercially available dry etch reactors nowadays operate at frequencies between 100 kHz and 13 MHz, and some even use microwave frequencies (~4 GHz).

1.5.3 Temperatures of Plasma Species

All the species within a plasma receive energy directly, or indirectly, from the applied electric field. Their energy distributions are close to Maxwellian, and consequently they can be considered to have a 'temperature'. The temperature T , of a plasma particle is often quoted in Kelvin, or converted to eV using

$$\text{Kinetic Energy} = (3/2) kT / e \quad (1.5.0)$$

where k is Boltzmann's constant and e is the electronic charge. The three main species types within a plasma (ignoring photons), namely ions, electrons and neutrals, all have different effective temperatures, which are dealt with separately below.

Since the plasma region is at equipotential, averaged over a whole RF cycle this region may be considered field free (see section 1.5.5). However the edges of the plasma oscillate with the applied RF, producing waves which propagate into the plasma. Charged particles can interact with these plasma waves and gain energy. The amount of energy a particle obtains in this fashion will depend upon its mass.

Electrons, with their small mass, respond quickly to these field fluctuations, gaining momentum rapidly after each successive collision with gas molecules. Moreover, electrons can also gain energy from the heating effect of reflections from the moving sheath boundary (see sections 7.2.1 to 7.2.4) or by acceleration of secondary electrons through the entire sheath region (see section 7.3). The electron temperature, T_e , is therefore very large, being typically 20,000 K or more ($kT_e \sim 2$ eV). Generally speaking, for electropositive gases T_e increases with RF power and decreases with increasing pressure [143]. The electron energy distribution is considered in more detail in the next section.

In contrast, **ions** can only receive a small amount of momentum directly from the electric field, and so they have an average Boltzmann temperature that is only a little higher than ambient. The ion temperature, T_i , is typically about 400 K (or $kT_i \sim 0.05$ eV).

Neutral gas molecules only gain energy inefficiently, usually via collisions with ions. Consequently, they remain essentially at the ambient room temperature, with the atom temperature, $T_a \sim 300$ K, and $kT_a \sim 0.04$ eV.

In certain circumstances however, particles can obtain kinetic energies much greater than these. Examples are (a) species formed by electron impact dissociation reactions, where

conservation of momentum allows the post-reaction products to fly apart with energies of up to a few eV (see section 4.7.7), (b) collisional backscattering of ions or neutrals from the sheath into the plasma region (see section 6.15), and (c) ions and neutrals in the sheath region can attain energies of several hundred eV (see chapters 5 and 6).

1.5.4 Electron Energy Distribution

It was mentioned earlier that the energies of particles in the discharge can be described by a Maxwell-Boltzmann distribution, but this will only apply to an assembly of particles in true thermal equilibrium. However, an RF discharge is in a non-equilibrium state. A consequence of this is that departures from the Maxwellian distribution may occur. For the relatively massive ions and neutrals, a Maxwellian distribution is a reasonable approximation. However, the electron energy distribution may be strongly influenced by this non-equilibrium effect. With this in mind, Druvestyn and Penning [144] calculated a theoretical distribution of energies for electrons moving in a weak electric field. Their theory predicts a distribution similar to the Maxwellian one, but with fewer electrons in the high energy tail. However experimental evidence indicates that the *real* electron energy distribution is much closer to Maxwellian than would be expected based on the Druvestyn and later models [145,146,149] (see fig.1.8 in section 1.3.4.4.6 for examples of electron energy distributions in EN and EP plasmas).

1.5.5 The Plasma Potential and Sheath Potential

One of the most important concepts in the description of electrical discharges is the idea of a *sheath* region surrounding any surface in contact with the plasma. It is the difference in the electrical potential between the plasma region and this sheath region that directly leads to positive ion bombardment of the surface, and hence forms the basis of the calculations described in Chapters 5 to 7. We need, therefore, to discuss in detail the form and magnitude of these potentials.

If an electrically isolated substrate is inserted into the plasma, it will initially be struck by positive ions and electrons. The flux of each species will be unequal as a result of the much higher speed of the electrons. The flux, J , of a species of mass m and density n is given by [47]

$$J = enc / 4 \quad (1.5.1)$$

where e is the electronic charge and c is the mean speed of the species given by

$$c = \{ 8kT / (\pi m) \}^{1/2} \quad (1.5.2)$$

with k = Boltzmann's constant and T = absolute temperature.

As a result of the much larger flux of electrons arriving at the substrate, it begins to charge negatively with respect to the plasma. This excess negative charge density around the substrate is called the space-charge, or *sheath*. The substrate will continue to charge negatively until the

electron flux is reduced by repulsion just enough to balance the ion flux.

Except around disturbances such as these, the remainder of the plasma is at equipotential. This potential is termed the *plasma potential*, $V_p(t)$, which oscillates with the applied RF voltage $V_0(t)$. The potential held by an isolated substrate in the plasma is known as the *floating potential*, V_p^0 , so-called since the potential ‘floats’ to a value sufficient to maintain an equal flux of positive and negative species. The potential difference between the floating potential and plasma potential ($V_p - V_p^0$) is the *sheath potential*. This is the magnitude of the energy barrier which an electron must surmount in order to reach the substrate. It is also the potential through which a positive ion is accelerated onto the substrate.

All surfaces in contact with the plasma are surrounded by a sheath region, including the electrodes and walls of the chamber. Most of these surfaces are usually grounded and so their corresponding sheath potentials at any instant in time are equivalent to the plasma potential. The powered electrode, however, is capacitively-coupled to a generator which provides a potential which oscillates on an RF timescale. Therefore, the powered electrode sheath potential can be very large (several hundred V) and will oscillate in magnitude with the applied RF. The sheath region will also expand and contract with the RF.

Since a sheath is a region over which a negative potential is dropped, electrons are rapidly expelled from the sheath. This loss of electron density in the sheath results in a reduction of electron impact excitation reactions in that region. Since such reactions lead to fluorescent emission from excited species, the sheath region does not glow as much as the plasma bulk. The substrate is surrounded by a comparatively *dark space*, a feature common to all objects in contact with the plasma. This includes electrodes, walls of the reactor, semiconductor substrates and Langmuir probe wires.

1.5.6 Voltage Distributions in RF Plasmas

For a capacitively-coupled RF plasma, such as is used for RIE processes and in the present work, the presence of a blocking capacitor between the RF generator and the plasma introduces the constraint that no net current can flow during one RF cycle. In other words, the net total charge flow per RF cycle to both anode and cathode must sum to zero. Also, in most RIE systems the grounded electrode (anode) has a much larger surface area (A_a) than the driven or powered electrode (cathode) area (A_c). The only way for the plasma to attain zero charge flow therefore, is to have very different sheath potentials at the cathode and anode. Consequently, the cathode charges up negatively until enough electrons are repelled for this constraint to be met. This results in a large negative *DC offset voltage* developing between the cathode and the plasma. This *DC bias* (V_{dc}) can be several hundred Volts and have a magnitude up to V_0 depending upon the value of A_c/A_a [148]. Song *et al* [148] have recently derived a relationship between this electrode area ratio and the sheath voltage ratios for an RIE etcher. This work has proved to fit experimental data very convincingly, and is beginning to supersede older, inadequate theories [137]. Moreover, the theory given by Song *et al* produces expressions for the DC bias and plasma potential using only readily measurable plasma parameters. Song *et al* obtained the following for some of the fundamental potentials in the plasma:

$$V_e(t) = V_0 \sin(\omega t + \phi) - V_{dc} \quad (1.5.3)$$

$$V_{dc} = V_0 \sin \left\{ \left(\frac{\pi}{2} \right) \left[\frac{1 - A_e}{1 + A_e} \right] \right\} \quad (1.5.4)$$

$$V_p(t) = (kT_e / e) \ln \left\{ \left[1 + A_e \exp(eV_e(t) / kT_e) \right] / \left[1 + A_e \right] \right\} + V_p^0 \quad (1.5.5)$$

with the floating potential given by [47]

$$V_p^0 = (kT_e / 2e) \ln \left\{ m_i / (2.3m_e) \right\} \quad (1.5.6)$$

where $V_e(t)$ = the voltage on the cathode, V_0 = the applied RF voltage, $A_e = A_c/A_a$, m_i = ion mass, m_e = electron mass, ω = frequency of RF, and ϕ = RF phase.

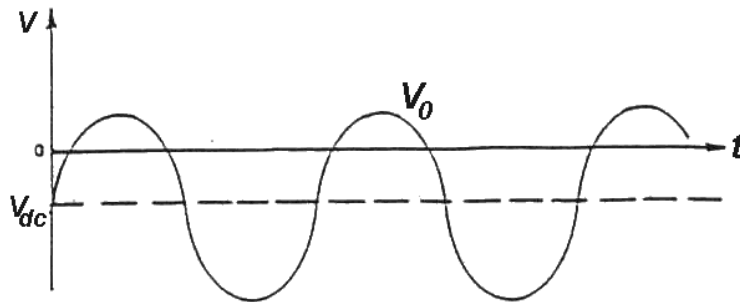


Fig.1.9. Variation of V_0 with time t for an RIE system.

Fig.1.9 illustrates the relationship between V_0 and V_{dc} . We note that the potential is positive for only a short fraction of each cycle, and it is only in this short period that electrons can strike the electrode. The time variation of the anode sheath potential (\sim plasma potential) and cathode sheath potential are given in fig.1.10. The cathode potential is much larger than the anode potential, and is greater than its minimum value for a larger proportion of the RF cycle. The anode potential is smaller and is in anti-phase to the cathode potential. The time-averaged potentials across the plasma are illustrated in fig. 1.11. The plasma potential is always the most positive potential in the chamber.

Chapter 1 - Introduction

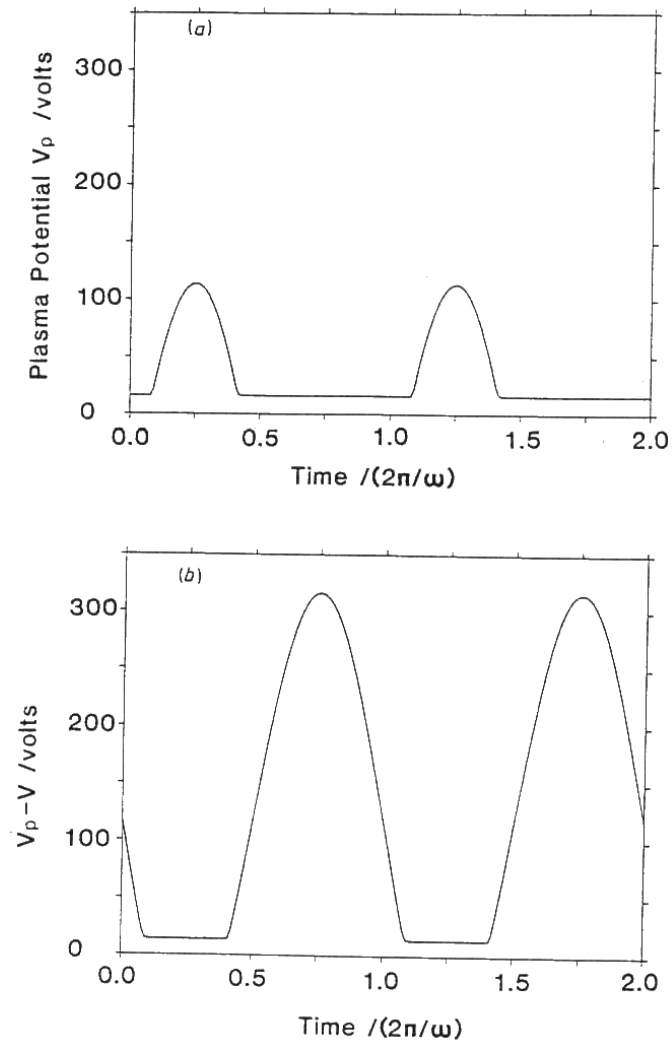


Fig.1.10. Variation of the sheath potential with time for (a) the anode and (b) the cathode for a 13.56 MHz RIE plasma (after Song *et al* [148]).

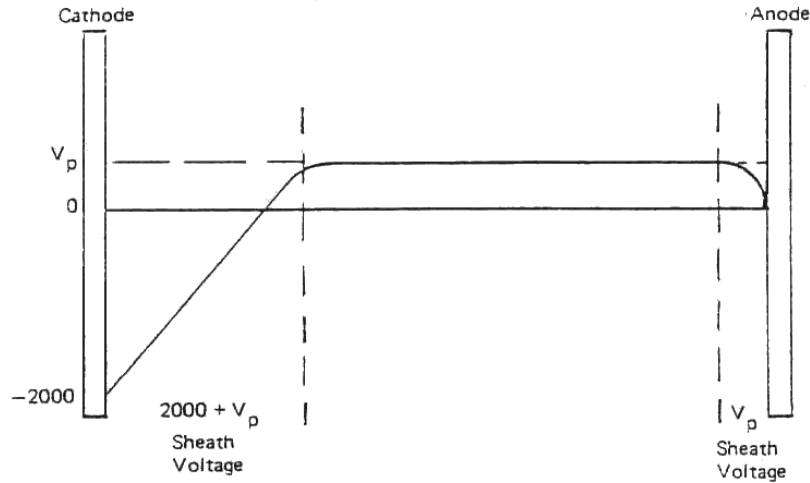


Fig.1.11. Time-averaged sheath potential versus location in an RIE reactor (after Chapman [47]).

1.5.7 Spatial Variation of the Sheath Potential

The variation of the potential V , with distance x , into the sheath is still uncertain. It is known that the form of the potential can be closely approximated using the assumption of a linear field [138,139]. However, this is unsatisfactory since it violates the flux conservation law stated in Poisson's equation [47]

$$d^2V/dx^2 = -\rho(x) / \epsilon_0 \quad (1.5.7)$$

This states that the second differential of the potential with respect to distance is simply proportional to the charge density $\rho(x)$ at the point x , the constant of proportionality being the inverse of the permittivity of free space, ϵ_0 .

A more satisfactory potential, derived in Chapman [47], is the *Child-Langmuir potential* given by

$$(4/3) V^{3/4} = (4J / \epsilon_0)^{1/2} (m_e / 2e)^{1/4} x \quad (1.5.8)$$

where J is the electron flux and m_e is the mass of the electron. This is often known as the *high vacuum version of the Child-Langmuir space-charge limited potential* [151,152].

At higher pressures, the passage of the electrons through the gas may be inhibited by collisions, and at sufficiently high pressure it may become *mobility-limited*. Under these conditions, the drift velocity v of the electrons is proportional to the electric field E , with the constant of proportionality being the *mobility*, μ . By substitution of $v = \mu E$ for the free-fall velocity of the electrons in the derivation of the Child-Langmuir potential [47], we obtain the *high pressure or mobility-limited version of the Child-Langmuir equation* [153]

$$V = (2/3) \{ 2J / (\epsilon_0 \mu) \}^{1/2} x^{2/3} \quad (1.5.9)$$

For RIE plasmas, the low pressure Child-Langmuir equation is usually taken as the best approximation, although other workers have produced modifications to this or developed alternative expressions [154-158].

1.5.8 The Bohm Criterion

This is a well-known phenomenon associated with DC sheaths which alters the nature of the plasma close to the sheath boundary [47]. The sheath does not end abruptly, but decays exponentially in a quasi-neutral transition region. This region has an electric field associated with it that accelerates ions up to an energy of about $(kT_e/2)$ eV before they enter the sheath proper. Also, it reduces the ion flux entering the sheath by a factor of about 0.6, and modifies the floating potential. The potential variation near an electrode therefore has the structure depicted in fig.1.12.

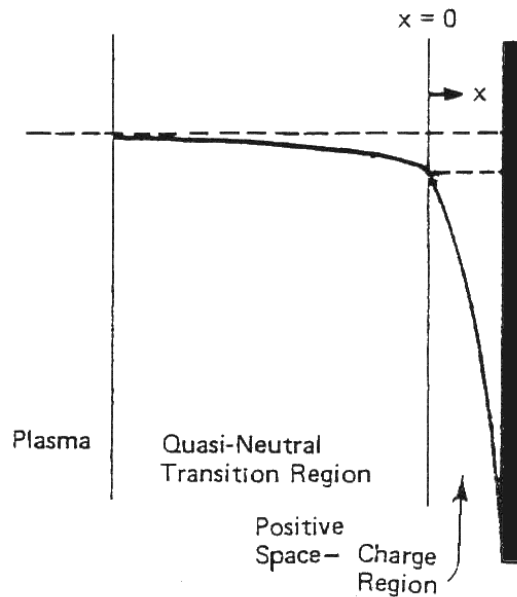


Fig.1.12. Potential variation near a negative electrode (after Chapman [47]).

However there are a number of problems associated with the standard derivation of the Bohm formulae. First, it is assumed that the ion temperature is zero, that is, the ions are all stationary. Second, there is a further assumption that there are no collisions within the sheath, which is reasonable for low pressure (<5 mTorr) plasmas, but invalid at higher pressures. Finally, the Bohm formulae for ion current derived in Chapman [47] does not explicitly include the cathode potential, as the author notes. Moreover, for sheaths oscillating at RF frequencies the pre-acceleration which the Bohm criterion proposes may not have time to take place before the quasi-neutral transition region is enveloped by the rapidly-moving sheath. The combination of these factors makes the topic of the Bohm criterion controversial when describing the details of plasma-sheath boundaries. This is discussed further in section 5.7.

1.5.9 Plasma Chemistry

Chemical reactions in the bulk of the plasma can play a fundamental role in determining the kinetic energies of species within the discharge. As such, we shall now briefly describe some of the major reactions that occur within typical RIE processes.

Plasmas are very complex in nature, and may be considered as a chemical 'soup' of ions, electrons, free radicals, stable molecules and photons. All of these constituents can interact with each other via a large number of complex chemical pathways, both in the gas phase and at the plasma-surface interface. Detailed descriptions of all of these processes are beyond the scope of this thesis and can be found in most modern textbooks on plasma chemistry [7,9,47] or other sources [30,31]. Therefore, we shall only emphasise those processes which are relevant to the present work.

The fundamental processes occurring within most low density plasmas are [9]:

(a) **Electron impact reactions**, such as

Excitation (rotational, vibrational or electronic)



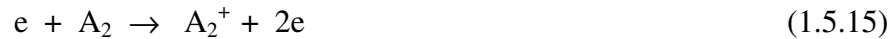
Dissociative attachment



Dissociation



Ionisation



Dissociative ionisation

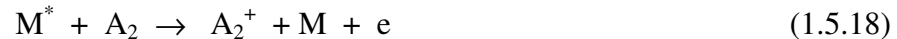


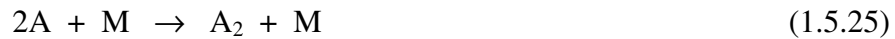
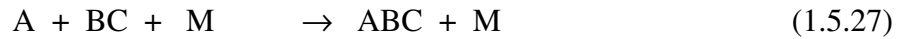
(b) **Inelastic collisions between heavy particles**, such as

Penning dissociation

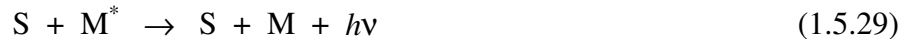


Penning ionisation



Charge transfer**Collisional detachment****Associative attachment****Ion-ion recombination****Electron-ion recombination****Atom recombination****Atom abstraction****Atom addition**

(c) **Heterogeneous reactions** (S = solid surface in contact with the plasma), such as

Atom recombination**Metastable de-excitation****Atom abstraction****Sputtering**

In all the above reactions, M is a third body, and asterisk denotes an excited state. Equations (1.5.11) and (1.5.13) are the ones especially relevant to the present work. In section 4.7.7 we explain how FPI techniques are used to distinguish between these two mechanisms as a candidate for the formation of excited Cl^* in a Cl-based RIE plasma.

1.5.10 Ion-Surface Interactions

For RIE etching, the bombardment of the semiconductor substrate surface by directional, energetic ions forms the basis for mechanisms of anisotropic etching. In Chapter 8 it will be shown that a detailed knowledge of these ion-solid interactions can be used to model sputtering profiles. We therefore now explain the background to the subject.

There are 10 main ways in which ions from the plasma can interact with surfaces, and these are illustrated in fig.1.13. A brief description of each of these interactions will now be given.

- (1) **Backscattering:** The incoming ion can be backscattered (reflected) from the surface. The trajectory of the backscattered ion will depend upon the exact nature of the ion-surface collision process. Both elastic and inelastic collisions can occur.
- (2) **Surface Dislocation:** The momentum of the incident ion may be sufficient to dislodge a surface atom from a weakly-bound position on the lattice and cause it to be relocated into a more strongly-bound position.
- (3) **Internal Dislocation:** Ions with high energies can penetrate deeply into the target and cause atomic dislocations in the bulk.
- (4) **Sputtering:** When ions transfer enough of their initial momentum to entirely free one or more atoms, these atoms can leave the surface and become sputtered.
- (5) **Implantation:** As ions penetrate into the target, they lose energy in collisional processes with target atoms. When the ion energy is expended, the ion will remain trapped or implanted in the target.
- (6) **Chemical Sputtering:** Chemical reactions between the ion and surface atoms can occur. As a result, new compounds can be formed on the surface which then leave as a gas. This is the basis for RIE.
- (7) **Charge Transfer:** The positive ion can gain an electron from the surface by an Auger Neutralisation process (see section 7.3.1.1.1) and be reflected as a neutral atom.
- (8) **Ion Adsorption:** Ions can become bound to the surface without being neutralised.
- (9) **Secondary Electron Emission:** High energy particle bombardment of the surface can lead to emission of electrons (see section 7.3).
- (10) **Secondary Ion Emission:** This occurs when surface atoms are excited to ionised states and then ejected.

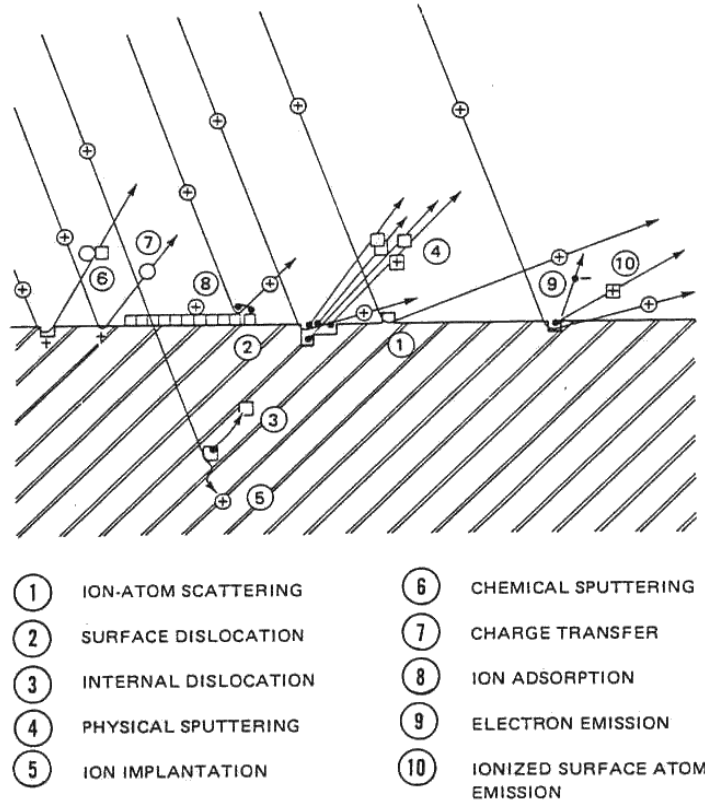


Fig.1.13. The main ion-solid interactions (after Brodie and Muray [239]).

The interaction of energetic ions with matter has been a subject which has received great theoretical and experimental attention since the turn of the century [200]. Indeed, it was the scattering of ions through Al foil that led Rutherford to develop a model of the atom [201]. An historical review of the study of ion-matter interactions is given in ref.[202]. Most of this work deals with very high energy ions, such as occur in particle beams or nuclear reactions, and so is of little use to RIE processing, where the ion energies rarely exceed 1 keV. A review of the ion-surface interaction processes that are relevant to RIE can be found in work by Zalm [203], Dielman [204] and Winters [205].

One of the major methods used to study these surface phenomena experimentally, especially in the presence of reactive gas molecules are ion beam techniques. Kolfshoten *et al* [206] and Oostra *et al* [207] studied Ar^+ ion-assisted etching of Si by Cl_2 using this technique, and concluded that the ion-surface interactions can be described by a collision cascade model. Park and Clay [208] used a theoretical model of this same reaction to calculate the product energy and angular distributions. They concluded that the main reaction products are Si and Cl together with some SiCl and SiCl_2 , which is consistent with experimental findings.

One of the most modern attempts to obtain a detailed description of ion-solid interactions was performed by Ziegler *et al* [202]. They wrote a Monte Carlo computer program called TRIM (short for Transport of Ions in Matter) which allows the stopping powers to be calculated for an ion of any mass (1-92 amu) in any amorphous solid (including compounds such as cement or photoresist). The program follows the trajectory of the ion within the solid as it collides with

the substrate atoms. It also calculates the full cascade of substrate atom trajectories, and provides a detailed analysis of the damage effects within the solid. It can calculate sputter yields for ions of any incident angle and energy, giving values which agree closely with experimentally observed results. Its simplicity and ease of operation has made it ideal for studying impact phenomena. It is for this reason that TRIM was chosen for sputtering simulation work (see section 8.2).

In later sections we shall return to look at some of these ion-surface interactions in greater detail. Chapter 7 includes a detailed description of secondary electron production, and Chapter 8 discusses in depth both ion backscattering and surface atom sputtering mechanisms.

1.6 Fabry Perot Interferometry (FPI)

In the present work we use FPI to study the kinetic energies of excited species in the bulk of an RIE plasma (see Chapter 4). Since FPI is a rather specialised technique, which is very unusual for the study of RIE plasmas, we shall now give a detailed introduction to the subject.

FPI is a technique that is used to study emission lines with ultra-high resolution. It has been used previously to measure very close splittings of spectral lines, such as occur in hyperfine structure and isotope shifts [110]. It has also been used for the determination of absolute length scales and the establishment of extremely accurate secondary standards of wavelength (relative to the Kr standard) [111,112]. Another important use is to measure the width and shapes of spectral lines yielding information about the temperature of the emitting species. Both H atom [104,105] and F atom emission [106] have been studied in this way. A Fabry Perot interferometer also forms the basic laser resonant cavity.

To date, there has only been one reported FPI study of RIE plasmas. Gottscho and Donnelly [109] used FPI to study the kinetic energy of F atoms in a CF₄ discharge. Their main aim was to determine the validity of using certain gases for actinometry purposes in different plasmas. They found that Ar emission gave a narrow line, and so concluded that excited Ar* was produced by electron impact of the ground state Ar atom. F atoms also gave the same result, and these workers concluded that actinometry was valid for the CF₄ system. They then tried to study Cl emission lines from a Cl₂/Ar discharge, but found that their Fabry Perot mirrors were inefficient at the longer wavelengths required. Therefore they used a high resolution spectrometer instead, which gave acceptable results, but which were not as detailed or as accurate as FPI would have given. These results showed that Cl gave a broadened linewidth, possibly indicating that a bond-breaking process was responsible for the production of excited Cl* atoms. Electron impact dissociation of Cl₂ was thought to be the mechanism responsible. One of the reasons that FPI was employed by us to study Cl atom energies, was to verify this finding, and to obtain a more accurate measurement of the behaviour and formation mechanism of excited Cl* in RIE plasmas.

1.6.1 FPI - *Modus Operandi*

A detailed theoretical account of the operation of a Fabry Perot (FP) interferometer can be found in most modern textbooks on optics [110,113]. Only a brief description will therefore be given here. In principle, the device consists of two plane, parallel, highly-reflecting surfaces

(mirrors or plates), separated by some distance, d . The enclosed air-gap, or cavity, varies from a few tenths of a mm to a few cm. If d is held fixed, the FP is called an *etalon*, otherwise an *interferometer*. The non-reflective faces of the plates are often made to have a slight wedge-shape (a few minutes of arc) to reduce the problems of interference patterns being produced between light reflected off the front and back surfaces of the plates.

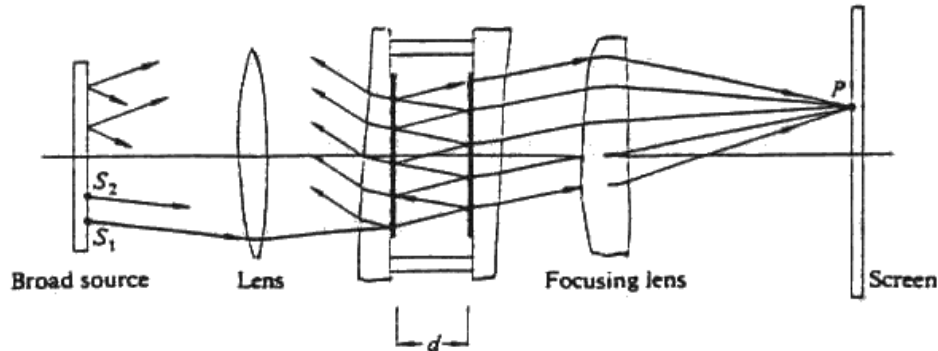


Fig.1.14.1. Basic Fabry Perot etalon (after ref.[113]).

Fig.1.14.1 shows the basic FP etalon. It is shown illuminated by a broad monochromatic source (such as a HeNe laser beam spread out to a diameter of a few cm). Only one ray emitted from a point S_1 on the source is traced through the etalon. Entering by way of the partially-silvered plate, the ray undergoes multiple reflections within the cavity. The transmitted rays are collected by a lens and brought to a focus on a screen. When the plane of incidence which contains all the reflected rays is considered, it is seen that light emitted from a different point, S_2 which is parallel to the original ray, but in its plane of incidence, will also form a spot at the same point P on the screen. The contribution to the intensity at P is the sum of all the irradiance contributions.

All of the rays incident on the gap at a given angle will result in a single circular fringe of uniform irradiance (see fig.1.14.2). With a broad diffuse source, the interference bands will be narrow concentric rings, corresponding to the multiple-beam transmission pattern (see fig.1.14.3).

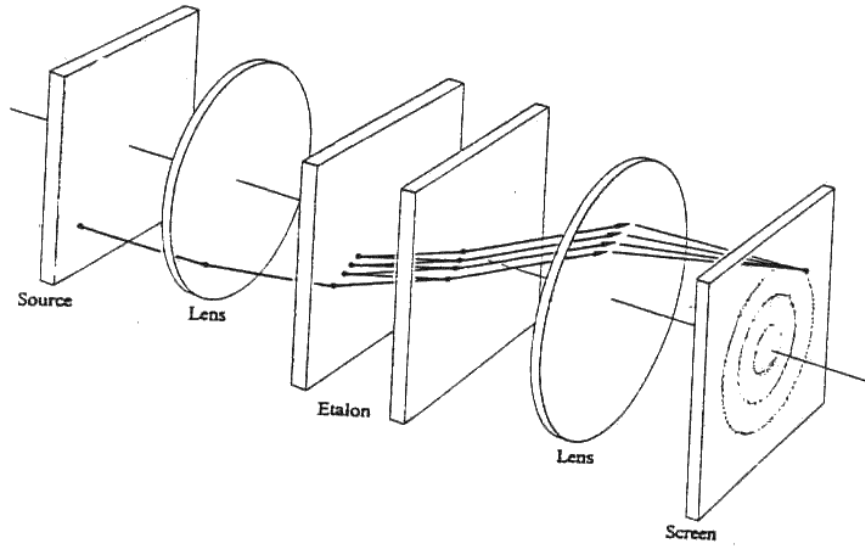


Fig.1.14.2. FP operation (after ref.[113]).

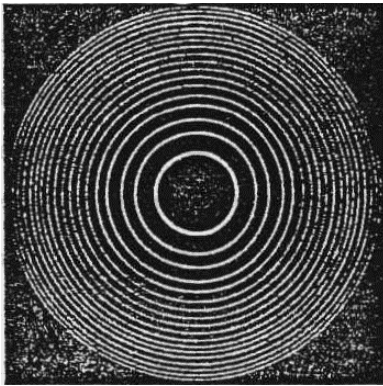


Fig.1.14.3. FP etalon circular fringes (after ref.[113]).

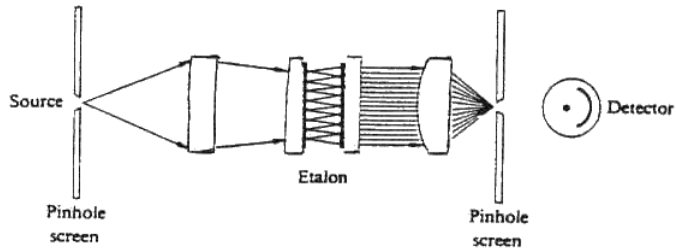


Fig.1.14.4. Central spot scanning.

1.6.2 FPI Spectroscopy

There are many possible ways to utilise FPI spectroscopically [111], but only the method used in this thesis will be detailed here. The technique utilised is called *central spot scanning*, and is depicted in fig.1.14.4. It uses a small pinhole aligned with the optical axis of the FP, which only allows the central spot of the interference pattern to reach the detector. The interference pattern is then scanned, causing the concentric rings to expand (or contract), the central spot changing in intensity as it alternates between a constructive interference fringe and a destructive interference fringe. Scanning is achieved in some FPs by altering the air pressure within the etalon. An alternative technique is to vibrate one FP plate through a distance of a few wavelengths of the light used. Piezoelectric mirror-mounts are used for this purpose, which

change their length, and therefore d , with an applied voltage. The voltage profile defines the mirror motion.

1.6.3 Basic FPI Terminology and Definitions

In order to understand FP operating procedures, it is necessary to give a brief overview of the terminology and definitions associated with FPI. The theoretical derivations for many of the following terms are given in standard sources [110,114].

For light of wavelength λ incident at an angle θ to a FP with mirror spacing d , the condition for constructive interference is

$$2nd \cos \theta = m \lambda \quad (1.6.1)$$

where n is the refractive index of air and m is the order of interference. The simulated output of the FP for various incident light source types is illustrated in fig.1.15.

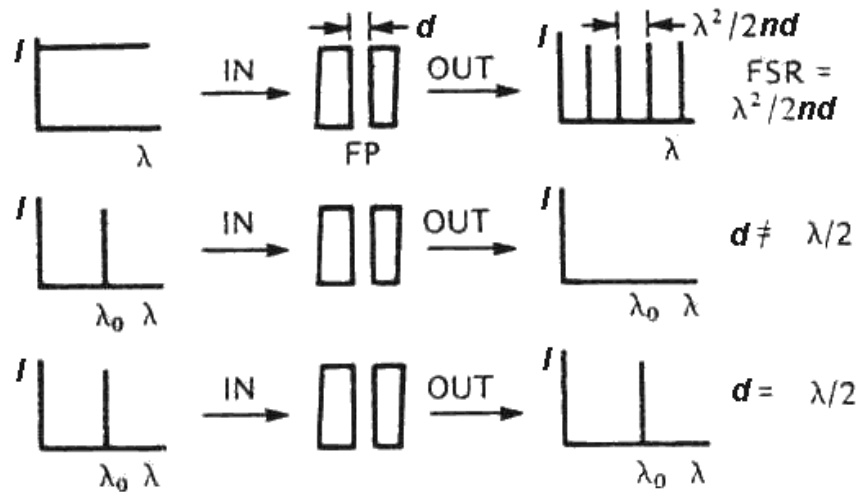


Fig.1.15. FP output for broadband and monochromatic output (after ref.[114]).

Working through the standard *Airey formulae* [113] we obtain the following:

(a) **Free Spectral Range (FSR):** The spectral display obtained when scanning a FP is repetitive, with each repeating unit being termed a *spectral order*. The range of wavelengths which can be displayed in the same spectral order without falling into consecutive orders is termed the *free spectral range* (FSR). The FSR in wavelength units is given by

$$\text{FSR} = \lambda^2 / (2nd) \quad (1.6.2)$$

(b) **Finesse (F):** This is the key measure of the FP's ability to resolve closely-spaced lines. It can be thought of as the effective number of interfering beams involved in forming the FP multiple-beam fringes. Each factor which reduces the overall finesse makes the resolving power

of the instrument worse. The four main factors which affect the finesse are:

- (i) **Reflectivity Finesse, F_R** : Since the mirror reflectivity R is less than one, losses will result which affect the FP resolution. This reflective finesse component is given by

$$F_R = \pi(R)^{1/2} / (1 - R) \quad (1.6.3)$$

- (ii) **Flatness Finesse, F_F** : This is the measure of the lack of parallelism and/or planeness of the mirrors. FP mirrors are usually specified by the manufacturers as having a flatness of λ / M , where M is the fractional wavelength deviation from planeness across the mirror aperture. The flatness finesse component is given by

$$F_F = M / 2 \quad (1.6.4)$$

- (iii) **Pinhole Finesse, F_p** : The presence of a pinhole in the system (*e.g.* in central spot scanning) can contribute significantly to the total finesse of the FP. Generally the smaller the pinhole diameter D_p , the better the finesse, although this will result in loss of light transmission, which can be a serious problem when dealing with small light signal levels. Pinhole finesse is given by

$$F_p = 4 \lambda L^2 / d(D_p)^2 \quad (1.6.5)$$

Here L is the focal length of the lens that focuses the light from the FP into the pinhole.

- (iv) **Diffraction Finesse, F_D** : This is the measure of the effect that the diameter of the limiting aperture has upon the FP output. The limiting aperture is often the diameter of the FP mirrors. In the case where a pinhole is employed in the optical system, the limiting aperture is the pinhole diameter. F_D is given by

$$F_D = 2(D_p)^2 / (\lambda nd) \quad (1.6.6)$$

- (v) **Total Finesse, F_T** : The net finesse is found by treating the component finesses as if they were parallel impedances

$$F_T^{-2} = \sum_i (F_i)^{-2} \quad (1.6.7)$$

(c) **Maximum Resolution**: The maximum resolution of the entire FPI system is a function of the total finesse, and is given by

$$\text{Max. Res.} = FSR / F_T \quad (1.6.8)$$

(d) **Other definitions**: Some other important features of a FPI system are given below, and these are all explained further in ref.[14].

- (j) **Throughput** - Defined as the transmission of a FP at resonance.
- (ii) **Etendue** - The light-gathering power of a FP.
- (iii) **Instrumental Function** - The spectral profile which would be observed with a purely monochromatic source.
- (iv) **Minimum Resolvable Linewidth** - The width (at FWHM) of the Instrumental Function.

1.6.4 Fabry Perot Design Considerations

There are several important parameters to consider when using FPI to study spectral lines accurately. Some of the general problems encountered when attempting ultra-high resolution spectroscopy can be eliminated by careful design of the FP instrument and apparatus. This is discussed below.

- (a) **Mechanical Stability:** The FP must be resistant to vibrations or knocks (such as footsteps or bumping the laboratory table). If the plates move by more than about 10 \AA due to these effects, the FP performance can be seriously affected. Mechanical creep is also a problem, causing misalignment of the plates. In general, mechanical stability is ensured by maintaining a high degree of design symmetry, using heavy spring loads against adjustment threads, incorporating hardened, polished adjustment interfaces, constraining all elements except for the desired motion, and using highly rigid construction materials.
- (b) **Thermal Stability:** The controlling parameters for this are the coefficients of expansion, thermal inertia and mechanical configuration of the FP component parts. Drifting of alignment by differential expansion of materials in the FP can be a major problem. This is usually minimised by using construction materials with low coefficients of expansion (such as Invar, Super-Invar, epoxies and PZT materials), and placing the FP inside a controlled thermal environment, such as an insulated box.
- (c) **PZT drive:** Piezoelectric tuning (PZT) is often used for alignment and scanning of the mirrors. Three independent PZT elements can be used to independently control the alignment by adjusting the voltage on each separately, or the tuning by adjusting all three simultaneously. This allows 'hands-off' adjustments, and makes automatic control of the FP possible.
- (d) **Mounting:** The two mirrors must be held in such a way that warping does not occur, while maintaining precise thermal and mechanical control. This must also be done in such a way as to reduce local distortions in the vicinity of the front surface. The three most commonly used methods are 3-point mounting, edge mounting and the Burleigh mounting, all of which are described in detail in ref.[114].

1.6.5 Optical Emission Linewidths and Lineshapes

FPI is used to study the widths and shapes of emission lines since these measurements often yield a great deal of information about processes occurring within a discharge. If an emission line is emitted at a central wavelength of λ_0 the observed line will have a definite lineshape and width due to several features of the source. The width of a line is usually defined as the full width at half maximum intensity (FWHM). A full treatment of lineshapes and widths is beyond the scope of this work, and the reader is directed to other sources for a more detailed exploration of the subject [110,115,116]. Only a brief résumé of the important phenomena will now be described, with an emphasis upon the phenomena relevant to FPI studies of RIE plasma sources.

1.6.6 Natural or Lifetime Broadening

Emission of light consists of a transition between two discrete energy levels. These levels cannot be infinitely narrow because the Uncertainty Principle in the form $\delta E \delta t \sim h/2\pi$ requires an energy spread of $\delta E \sim h/(2\pi \delta t)$, where δt is the mean lifetime of the upper state. This broadening is generally insignificant for transitions of long lifetime, but becomes important for transitions from states that have lifetimes shorter than ~ 1 ns. Most emission lines observed from RIE plasmas have lifetimes > 1 ns, and so lifetime broadening can usually be ignored.

1.6.7 Doppler Broadening

This is a result of the well-known ‘Doppler Effect’ which gives an apparent shift in wavelength of the signal from a source moving towards or away from the observer. Motion towards the observer causes a decrease in wavelength (blue shift), and motion away causes an increase (red shift). Even in a ‘stationary’ light source (such as a plasma), the emitting atoms are moving, and any component of velocity away from or towards the observer gives a red or blue shift, accordingly. A large number of atoms having different velocities will emit a spread of wavelengths, and produce a broadened line. If the gas is in thermal equilibrium at a temperature T , the distribution of atomic and molecular velocities is given by the well-known Maxwell-Boltzmann distribution. The linewidth resulting from a gas having this velocity will be a *Gaussian*, with a profile given by [110]

$$I = I_0 \exp\left\{ -c (v_0 - v) / (v_0 \alpha) \right\}^2 \quad (1.6.9)$$

where I_0 is the maximum intensity at a central frequency ν_0 , c is the speed of light and α is the most probable velocity from the Maxwell Boltzmann distribution, given by

$$\alpha = (2RT / M)^{1/2} \quad (1.6.10)$$

with R being the gas constant, M the molar mass of the emitting species and T the equilibrium gas temperature. Converting the equation to wavelengths [165], we have

$$T = \left\{ c \delta\lambda / 2 \lambda \right\}^2 M / (2R \ln 2) \quad (1.6.11)$$

which allows the calculation of the temperature of the emitting species from its Gaussian FWHM, $\delta\lambda$.

1.6.8 Pressure Broadening

Interactions between an emitting species and a nearby particle (atom, ion or electron) can perturb the energy levels involved in the transition, introducing a degree of energy uncertainty and hence broadening the line. These perturbations form the basis of so-called *impact theory* approximations, which allow lineshapes to be calculated [110]. As the pressure increases there is more opportunity for perturbation effects (collisions) to occur, consequently the linewidths of spectral lines increase, hence the name *pressure broadening*. The line profile resulting from this effect is called *Lorentzian*, and is similar in appearance to the Gaussian, except that it does not fall off as rapidly in the wings. At two FWHMs from the centre a pure Doppler profile has dropped to $\sim 0.2\%$ of the peak intensity, whereas a pure Lorentzian profile has dropped to only $\sim 6\%$. Therefore, detailed examination of the wings of an observed lineshape can often differentiate between pressure broadening and Doppler broadening effects. The Lorentzian line profile is given by the expression [113]

$$I^2 = f_0^2 / [4\{(\omega - \omega_0)^2 + \gamma^2/4\}] \quad (1.6.12)$$

where I is the line intensity governed by the normalisation factor f_0 , γ is the FWHM and ω is the mean frequency. A comparison of Gaussian and Lorentzian lineshapes is given in fig.1.16.

Often the spectral line has a shape that is a combination in some proportion of a Gaussian and Lorentzian profile. The resulting profile is obtained by ‘folding’ together the two profiles, and is termed a *Voigt* profile [110].

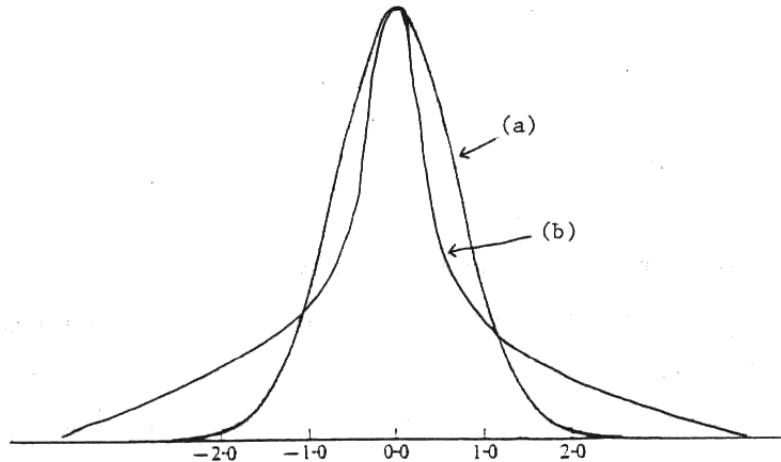


Fig.1.16. Examples of spectral lineshapes observed in optical emission spectroscopy. (a) Gaussian, (b) Lorentzian. The x -axis is calibrated in steps of the Gaussian FWHM.

1.6.9 Isotope Effects

Due to conservation of momentum, a spectral line emitted from an atom is slightly dependent upon the mass of the atom. Isotopes with differing masses therefore give rise to spectral lines at slightly different wavelengths. A 'single' spectral line can often be really composed of a very closely spaced multiplet of lines, with each component line having an intensity proportional to the relative abundance of the relevant isotope. With poor resolution, the multiplet may not be resolved, and the line will appear broader than it should. The splitting due to the effect of two isotopes of mass M_1 and M_2 is given by [117]

$$\bar{\delta\nu} = \{m_e \delta M / (M_1 M_2)\} \bar{\nu} \quad (1.6.13)$$

where $\bar{\delta\nu}$ is the peak separation in wavenumbers, m_e is the electronic mass, δM is the difference in mass between the isotopes and $\bar{\nu}$ is the emission wavenumber in cm^{-1} . The isotope of greater mass has the higher wavenumber. For most atomic species which have isotope masses only a few amu apart, the splitting of a spectral line is negligible compared to Doppler broadening.

1.6.10 Hyperfine Effects

Nuclei which have non-zero spin can interact with the electronic motion of the emitting atom via a coupling of their angular momenta and cause a splitting of the electronic energy levels [108]. Consequently, emission lines will be split into multiplets, although this splitting will be very small. Under poor resolution the emission lines will appear as a broadened singlet of irregular lineshape. Hyperfine splitting is usually negligible in comparison with Doppler broadening, but for certain nuclei it may warrant consideration (see section 2.10.10.3).

1.6.11 Stark Broadening

Charged particles in a plasma have associated electric fields. As the plasma density increases, these fields can become large enough to interact with the energy levels of polar molecules by distorting the electron clouds around the molecule. Local fields can polarise non-polar molecules so that these too may be subject to the *Stark effect*. Any photon emitted from the affected molecule will have a slight uncertainty about its energy, resulting in a broadened linewidth [118]. Usually, very high electric fields are needed to obtain a significant Stark broadening [119]. An example of this is given by Puric *et al* [107], who measured the Stark widths of F atom emission lines in a high power discharge. For typical RIE discharges the plasma density and electric fields are too low to make Stark broadening significant (see section 4.7.6).

1.6.12 Electron Resonance Broadening

Free electrons in a plasma resonate at a particular frequency with the so-called plasma waves (see section 1.5.3). A light beam passing through the plasma will interact with these oscillating electrons and be scattered. Any light scattered sideways will be broadened in proportion to the energy of these electrons [118]. For low power plasmas (*i.e.* ones with low electron temperatures), such as RIE plasmas, this effect is usually negligible.

1.6.13 Self Absorption and Self Reversal

A photon emitted at one point in a diffuse source may be reabsorbed by another atom before it has chance to escape from the source. This photon may be lost as a contribution to the spectral line since it could decay by another route [120]. Since the probability of emission is greatest in the centre of the peak, the probability of reabsorption is also greatest at the centre of the peak. This reduces the intensity of the observed spectral line proportionately more in the centre of the peak than at the edge, altering and flattening the lineshape and hence altering the observed linewidth. This effect can even make the line self-reverse, so that it appears to be a doublet. This is discussed in detail in section 4.7.3.

1.6.14 Instrumental Effects

The apparatus used for the observation of spectral lines (spectrometer, Fabry Perot, lenses, etc.) will never be perfect, and some distortion of the lineshape will result. This can often be a major factor when observing spectral lines with high resolution [100]. This so-called *instrumental factor* becomes important when the maximum resolution of the apparatus is comparable to the linewidth of the emission line(s) being examined. Poor resolution apparatus will artificially broaden a line or alter its lineshape. Often the linewidth broadening due to the apparatus can be calculated and then deconvoluted from the observed linewidth in order to obtain the true value. The procedure for this is described in section 2.10.10.1.

1.7 Ion Energy Analysis

A major part of the present work concerns the calculation of the energy of ions as they travel through the sheath regions to strike the electrodes of RF reactors. These calculated ion energy distributions (IEDs) are then compared to experimental observations in sections 5.4, 5.9.2 and 6.8. Therefore, we now present a brief introduction to the topic of ion energy analysis, firstly in terms of experimental techniques, and then a review of the theoretical work that has been done in this field. The review presented in these two sections is only intended as an introduction to IEDs. Some workers' experimental and theoretical studies shall be presented in later Chapters, where they will be discussed in detail and in the context of the present work.

Chapter 1 - Introduction

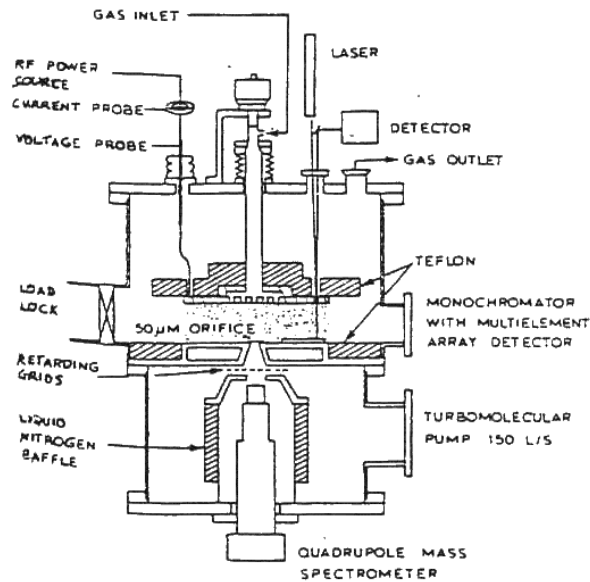


Fig.1.17. Ion energy analysis using a quadrupole mass spectrometer (after Thompson *et al* [124]).

Experimental ion energy analysis generally involves drilling a small hole in the electrode through which ions can pass into a detector outside the plasma. The ion detector usually consists of a set of grids to collimate the ions and repel secondary electrons, followed by a mass discriminator. The earliest detector was a simple quadrupole mass spectrometer [122-124], an example of which is shown in fig.1.17. This provides accurate ion energy analysis, but has the disadvantage of being expensive and unwieldy, and difficult to attach to an RIE reactor. In response to this, smaller, more versatile ion detectors have been designed [125-133]. A typical example is the parallel plate energy analyser used by Kuypers [131] (see fig.1.18), which uses an electric field on a pair of plates to deflect ions of different masses onto a Faraday cup detector. An RFA detector uses a Retarding Field Analysis technique to obtain ion energies [127] (see fig.1.19.1 and 1.19.2). This detector contains a spherical ion collector consisting of a large number of electrically isolated annular rings. This arrangement allows the angular distribution of ions to be measured as well as their energy.

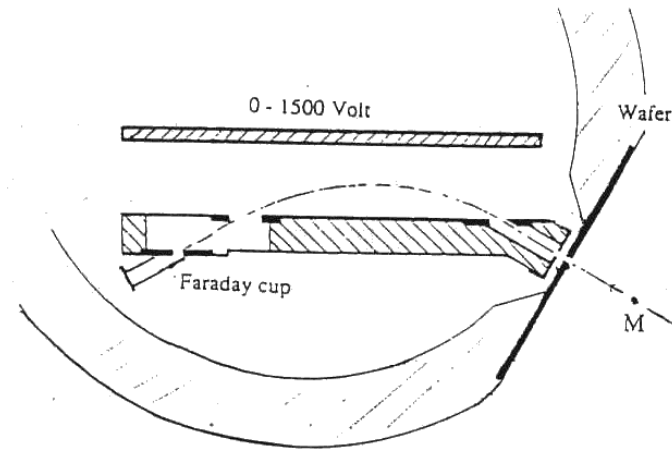


Fig.1.18. Schematic diagram of Kuypers' parallel plate analyser [131] inside a powered cylindrical electrode.

The first use of ion analysis for RF systems was by Coburn and Kay [121] who used a mass spectrometer to study ion bombardment of the anode. With this apparatus they obtained one of the first ion energy distributions (IEDs) for ions of different masses. The IEDs they obtained exhibited the now-familiar double-peaked shape (see section 5.2.2). These IEDs were found to show that the peak separation was inversely proportional to the square root of the ion mass. Most other experimental IED measurements to date have been performed for low pressure (<10 mTorr) inert gas plasmas, with IEDs often only observed on the grounded electrode for simplicity. Although these give an insight into the nature of ion trajectories in RF reactors, they are of little practical benefit since RIE etching uses pressures about 10 times higher than that used in IED measurement experiments. Moreover, the important electrode for IED experiments is the cathode, since the substrate is placed there in RIE to experience maximum ion bombardment.

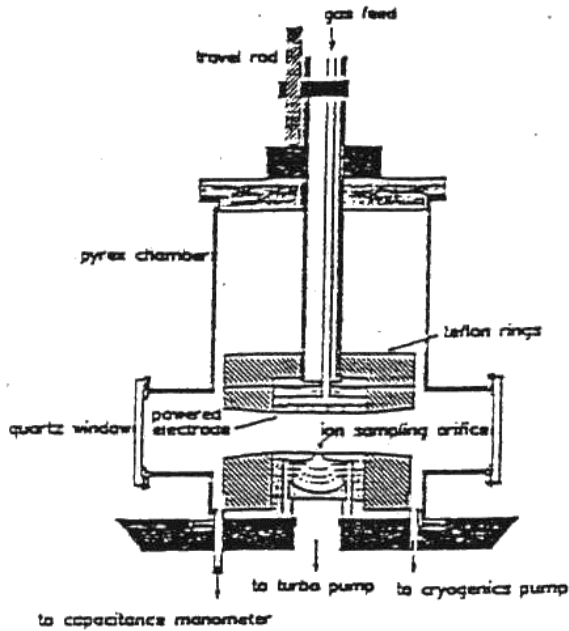


Fig.1.19. 1. Schematic of the experimental apparatus used in ion bombardment energy and angle measurements. Plasma is located between two 3"-diameter electrodes with the ion analyzer placed beneath the lower, grounded electrode. (After Sawin *et al* [127]).

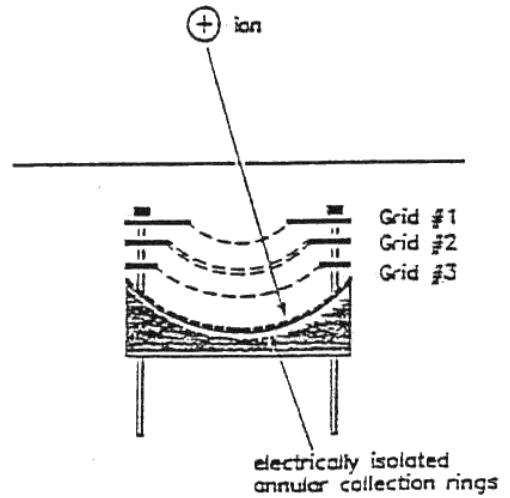


Fig.1.19.2. Detailed schematic of the ion bombardment energy and angle analyzer. The analyzer consists of three spherical grids for repelling ions or electrons and a spherical ion collector with electrically isolated annular rings. (After Sawin *et al* [127]).

Notable exceptions to this have been Thompson *et al* [124] who measured the IEDs of 'real' process gases such as SF₆, CFC₁₃ and CF₃Br, and Sawin *et al* [127] who measured IEDs and angular distributions in high pressure Ar plasmas. Kuypers [131,134] has measured IEDs for Ar, Ar/H₂ mixtures, CF₄ and O₂ plasmas on the cathode of a concentric cylinder reactor at low pressures. He has also measured an Ar IED at a typical RIE working pressure of 39 mTorr. We shall return to the results from these and other workers in section 5.4, when comparing simulated IEDs with experimental data.

1.7.1 Theoretical Studies of IEDs

In order to understand the IEDs obtained by the above workers, a few theoretical studies have been performed on the nature of ion trajectories as they pass through the sheath potential [135-141]. Most of this work deals only with low pressures, where the sheath may be considered collisionless. Failing accurate descriptions of the time variation of the sheath potential, most of these workers have used crude approximations, or dealt with time-averaged fields. Since more realistic models of the sheath potential are now available [148], accurate calculations of ion trajectories are now possible, and these form the basis of Chapters 5 and 6.

The first attempt at modelling ion trajectories was by Davis and Vanderslice [153], who

simulated Ar IEDs at the cathode in a high pressure plasma, but included only charge exchange effects (see section 6.4). The accuracy of their results was limited by neglecting momentum exchanging collisions. Also, they only simulated IEDs in DC discharges.

Zarowin [269,270] has estimated average quantities for the directed and random energies of ions passing through a sheath with many collisions, although, again, only charge exchange effects are considered. His assumption of a fully developed distribution (which will only occur at very high pressures, say > 500 mTorr) voids the applicability of these results to RIE plasmas where pressures are typically < 100 mTorr.

One of the most promising IED simulations to date was performed by Kushner [138]. He used a Monte Carlo approach to simulate IEDs, assuming again that charge exchange dominates the collisional interactions. His analysis included the effects of charge exchange processes upon ion energy and directionality, and the effects of RF sheath fields and thicknesses on the IED in the absence of collisions. Our model for ion trajectory calculations (described in Chapter 5) resembles Kushner's model in outline, except that we use the more realistic expressions for the plasma potentials derived by Song *et al* [148] rather than Kushner's assumption of an oscillating linear field.

Thompson *et al* [139] extended Kushner's work to calculate IEDs in both DC and RF sheaths. They consider *both* charge exchange and scattering effects, and use a $r^{-9} + r^{-6} + r^{-4}$ ion-neutral interaction potential for the scattering calculations. As with previous IED simulations through RF sheaths however, their description of the time-varying sheath potential is only approximate. They use both linear field and uniform field approximations for the sheath region, neither of which are an accurate representation of reality. Thompson *et al*'s work is discussed further in Chapter 6 when a model for ion collisions within the sheath is presented.

Sawin *et al* [127] have extended the Monte Carlo program used by Thompson *et al* to simulate IEDs experimentally observed at the anode of RF discharges. They directly compare IEDs seen in their reactor to simulations using parameters determined from the measured plasma conditions. These IEDs were obtained for pressures ranging from 10 to 500 mTorr. They also measure and simulate the angular distributions. Although their calculated IEDs bear an overall qualitative resemblance to the observed ones, the agreement is not very accurate in terms of obtaining the energies and positions of the various peaks in the spectrum. This discrepancy increases with increasing pressure, until by 500 mTorr there is no resemblance between the simulated and experiment IEDs. We shall discuss Sawin *et al*'s work in some detail when we deal with high pressure ion trajectory simulations in section 6.8.

Vallinga [135] has recently modelled RF sheaths in great detail and has derived an expression for the shape of the IED based on measurable plasma conditions. His work includes a useful expression for the IED peak separation which is detailed further in section 5.2.6.2.
